N.I.

AM–BASEBAND TELEMETRY SYSTEMS

Volume 1: Factors Affecting a Common Pilot System

by

RICHARD S. SIMPSON
WILLIAM H. TRANTER

February, 1968

TECHNICAL REPORT NUMBER 10

COMMUNICATION SYSTEMS GROUP

BUREAU OF ENGINEERING RESEARCH

UNIVERSITY OF ALABAMA UNIVERSITY, ALABAMA

AM-BASEBAND TELEMETRY SYSTEMS

Volume 1: Factors Affecting a Common Pilot System

by

RICHARD S. SIMPSON
WILLIAM H. TRANTER

FEBRUARY, 1968

TECHNICAL REPORT NUMBER 10

Prepared for
National Aeronautics and Space Administration
Marshall Space Flight Center
Huntsville, Alabama

Under

Contract Number NAS8-20172

Communication Systems Group
Bureau of Engineering Research
University of Alabama

ABSTRACT

An analysis of the coherent demodulation in SSB/FM and DSB/FM telemetry systems, having demodulation carriers synthesized from a common pilot, is performed. The analysis concerns demodulation when the entire baseband, including the pilot, is perturbed by tape recorder wow and flutter. The errors present in the demodulated waveform are analyzed, which results in approximate expressions for the error magnitudes. Also, the effect of additive gaussian noise on the pilot is analyzed. The nature of the resultant errors is discussed, and the magnitudes of the errors are expressed as a function of the signal-to-noise ratio. A set of Appendices is included which outlines related work.

ACKNOWLEDGEMENT

The authors would like to express their appreciation to the Telemetry Systems Branch, Marshall Space Flight Center, for the support of this work. In particular, Mr. Walter O. Frost and Mr. Frank H. Emens have contributed significantly to this work through the many discussions which were held at MSFC.

TABLE OF CONTENTS

LIST OF ILLUSTRATIONS

LIST OF SYMBOLS

ω_i	instantaneous frequency
ω_m	modulating frequency
ω_n	Channel N carrier frequency
ω_p	pilot frequency
ω_c	carrier frequency
ω_o	master oscillator frequency
$e_{DSB}(t)$	DSB signal
$e_{SSB}(t)$	SSB signal
$e^r_{DSB}(t)$	DSB signal at recorder output
$e^r_{SSB}(t)$	SSB signal at recorder output
$e_{in}(t)$	input signal
$e_r(t)$	recorded signal
$e_{out}(t)$	output signal
$e_{df}(t)$	data channel filter output
$e_{pf}(t)$	pilot filter output
$e_U(t)$	upper sideband signal
$e_L(t)$	lower sideband signal
$e_{sc}(t)$	synthesized demodulation carrier
$e_{dn}(t)$	Channel N demodulated output
$\mu(t)$	instantaneous phase deviation
$\dot{\mu}(t)$	instantaneous frequency deviation

$h(t)$	time-base error
$g(t)$	flutter
$\varepsilon(t)$	demodulation error signal
$\overline{\varepsilon^2(t)}$	mean-square value of $\varepsilon(t)$
$\theta(t)$	phase perturbation of pilot due to flutter
$\frac{\omega_n}{\omega_p}\theta(t)$	phase perturbation of Channel N carrier due to flutter
$v(t)$	instantaneous tape velocity
V	mean tape velocity
f_c	filter center frequency
$p(x)$, $q(x)$	probability density function of x
σ_x^2	variance of x
σ_x	standard deviation of x
$n(t)$	noise signal
N	channel number
z	signal-to-noise ratio
S_n	slope of the phase characteristic of the data channel filter
S_p	slope of the phase characteristic of the pilot channel filter
K	constant
$H(\omega)$,$Y(\omega)$	network transfer functions
$\phi(\omega)$	network phase response
$\lvert H(\omega)\rvert$, $\lvert Y(\omega)\rvert$	network amplitude response

I. INTRODUCTION

In SSB/FM and DSB/FM telemetry systems using suppressed carrier modulation, coherent demodulation is required; therefore, demodulation carriers must be synthesized. Several problems associated with the synthesis of demodulation carriers from a pilot signal are explored in this report.

An idealized SSB baseband spectrum and the basic scheme for demodulating SSB and DSB baseband signals are shown in Figures 1-1 and 1-2, respectively. The channel filters select the spectra of the channels to be demodulated and pass these signals to the product demodulators. If a data spectrum was translated to its baseband position by multiplication by a carrier, cos $\omega_n t$, proper demodulation requires that this carrier be present, with the proper phase relationship, at the demodulation carrier input to the product demodulator. This process requires careful attention, and if the baseband spectrum is perturbed in some manner, complications arise which lead to demodulation error.

In this report two such perturbations are studied. The first results from the baseband being recorded on an analog tape recorder. Upon playback the baseband spectrum is found to be perturbed by the wow and flutter inherent in the recorder. The effect of this perturbation and a method for its minimization is investigated. The second perturbation is caused by the pilot being subjected to additive baseband noise. This results in phase jitter of the pilot, which leads to demodulation error. The magnitude of the phase jitter is determined as a function of the pilot signal-to-noise ratio.

The appendices may be helpful to the reader in following certain of the developments.

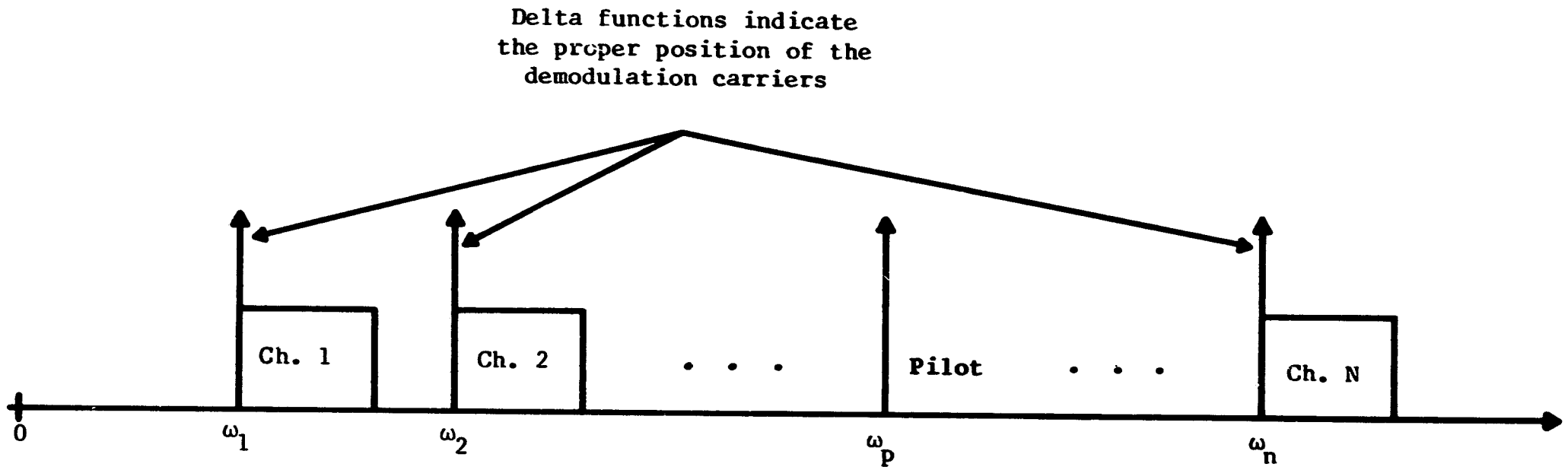

Figure 1-1 SSB Baseband Spectrum

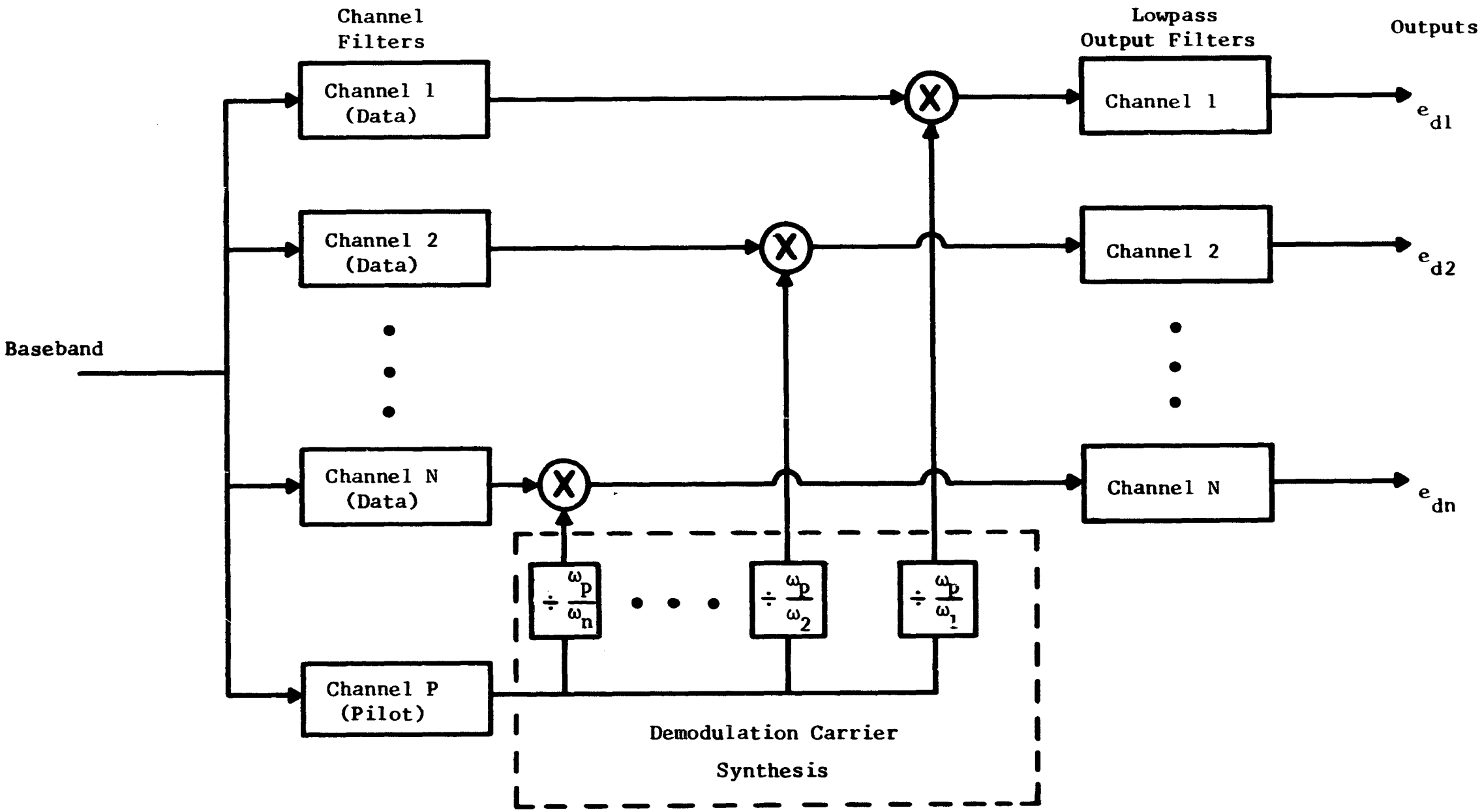

Figure 1-2 Baseband Demodulation Scheme

II. SYSTEM MODEL

The analysis of the effect of tape recorder perturbations on demodulation carrier synthesis requires that a suitable model of the AM portion of the system be developed. By including the modulation process as well as the demodulation process in the model, a clear understanding of the system is obtained. The model is used to determine the effect of tape recorder wow and flutter on an SSB system in Chapter III and a DSB system in Chapter IV.

A. Representation of Wow and Flutter

Wow and flutter, hereafter called flutter, arise from variations in the instantaneous speed of the tape across the record and playback heads in an instrumentation recorder. The major effect of these speed variations is to introduce a time-base error (TBE) in the signals which the recorder processes.[1] In other words, if a signal $e_s(t)$ is recorded, the recorder output, upon playback, may be approximated as

$$e_o(t) = e_s\left[t + h(t)\right], \tag{2.1}$$

where h(t) represents the composite TBE due to both record and playback flutter. It is shown in Appendix A that if the peak value of flutter is small, (2.1) may be used to describe both pre-detection and post-detection recording.

In order to formulate a more useful representation for a signal which has been perturbed by the recording process, a signal expressible by a sum of sinusoids will be considered. If the signal

$$e_s(t) = \sum_{j=1}^{n} \sin \omega_j t \tag{2.2}$$

---

[1] Superscripts refer to numbered references.

is recorded, the recorder output can be represented as

$$e_o(t) = \sum_{j=1}^{n} \sin \omega_j \left[t + h(t) \right] . \tag{2.3}$$

By defining

$$\theta_j(t) = \omega_j h(t), \tag{2.4}$$

we may write

$$e_o(t) = \sum_{j=1}^{n} \sin \left[\omega_j t + \theta_j(t) \right] . \tag{2.5}$$

Thus, the effect of the recorder is to impart a phase perturbation to each of the components in the recorded spectrum. Each of these perturbations is in phase and has a magnitude directly proportional to the recorded frequency.

B. Development of the Model without the Recorder

The first step in developing a model for the system will be to formulate a representation for the airborne carrier synthesis portion of the system. There are many ways that the original carriers can be synthesized, and one possible method is described in Appendix B. The results of this appendix indicate that if the carriers are to be harmonically related, they may be synthesized from a master oscillator running at a properly selected frequency ω_o. The Channel N carrier is synthesized by dividing ω_o by ω_o/ω_n, yielding the frequency ω_n. The pilot frequency, ω_p, results from dividing the master oscillator frequency by ω_o/ω_p.

After the carriers are synthesized, they are modulated by the information carrying signals. If

$$e_n(t) = \cos \omega_n t \tag{2.6}$$

and

$$e_m(t) = 2 \cos \omega_m t \tag{2.7}$$

represent the Channel N carrier and the modulating signal, respectively, the modulator output is

$$e_{DSB}(t) = \cos\ (\omega_n + \omega_m)t + \cos\ (\omega_n - \omega_m)t \qquad (2.8)$$

for DSB modulation and

$$e_{SSB}(t) = \cos\ (\omega_n + \omega_m)t \qquad (2.9)$$

for SSB modulation. The decision to work with the upper sideband is arbitrary.

After the individual carriers have been modulated by the information carrying signals, they are added with the pilot to form the baseband. The resulting signal is then transmitted through an rf channel to the ground station. The assumption is made that no error is introduced by the rf portion of the system.

The first elements in the AM portion of the ground station are the channel filters which select the channels to be demodulated. As shown in Figure 2-1, the outputs of the channel filters are passed directly to the product devices which perform coherent demodulation. The other inputs to the product demodulators are the demodulation carriers which are synthesized from the pilot. This synthesis process is much like the process shown in Appendix B except that the pilot having a frequency of ω_p replaces the master oscillator. Thus, the demodulation carrier for Channel N may be synthesized by dividing the pilot frequency by ω_p/ω_n. A low-pass filter to remove the $2\omega_n$ term completes the system.

The model for the AM portion of the system is shown in Figure 2-1 for the case where the tape recorder is not used. For simplicity only a general Channel N is shown. The problem now is to incorporate into the model the effect of a baseband recorder.

C. The Model with the Recorder

The pilot, after being recorded, will assume the form

$$e_p^r = \cos\left[\omega_p t + \theta(t)\right] , \qquad (2.10)$$

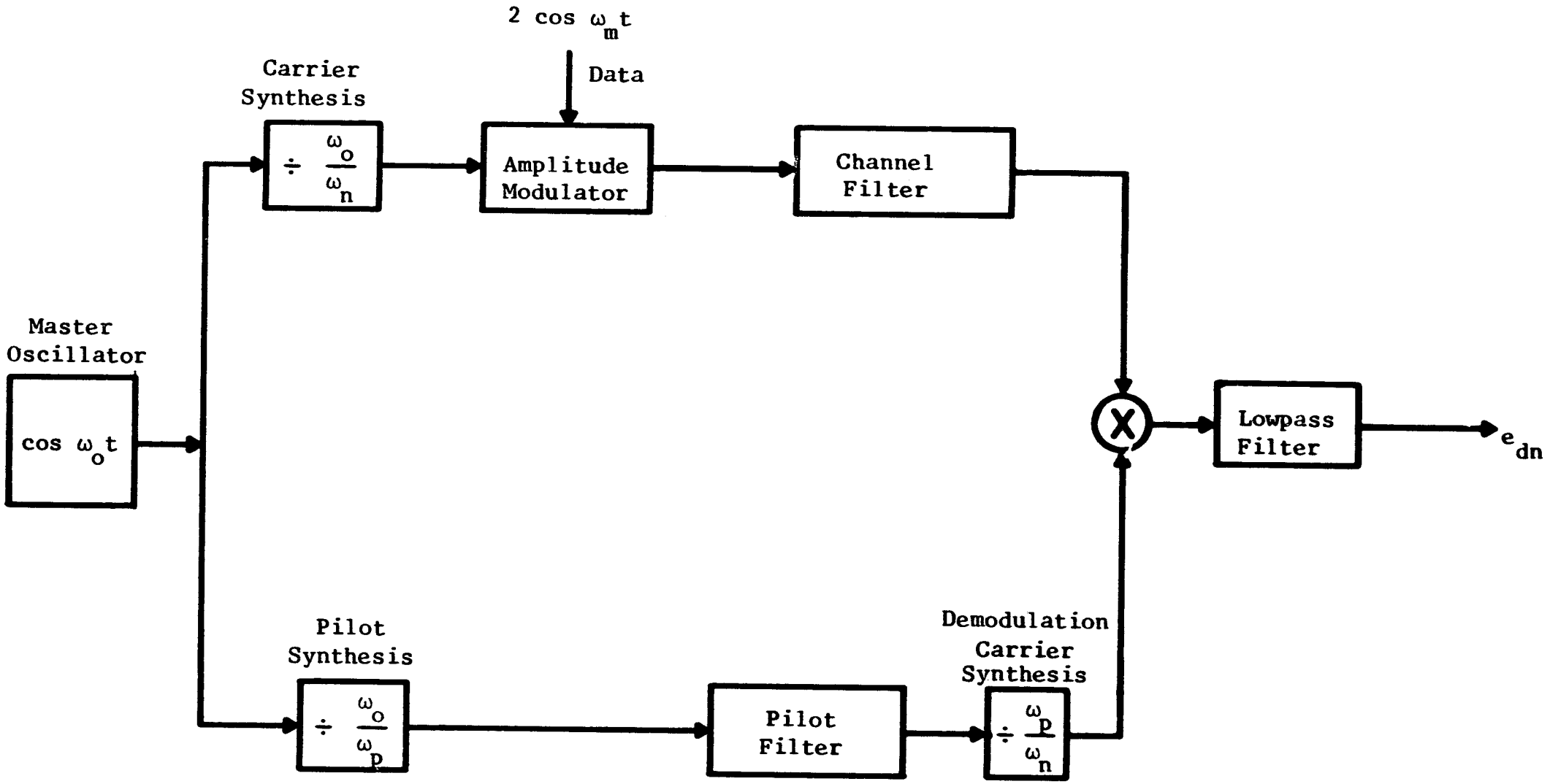

Figure 2-1 System Model without Tape Recorder

where $\theta(t)$ represents the phase perturbation of the pilot due to recorder flutter. For convenience all flutter perturbations are referenced to the pilot. Since the perturbation imparted to a signal by the recording process is proportional to recorded frequency, the phase perturbation imparted to the frequency $(\omega_n + \omega_m)$ will be

$$\frac{\omega_n + \omega_m}{\omega_p} \theta(t).$$

Therefore, after the SSB signal given in (2.9) is recorded and played back, the expression describing it will be

$$e^r_{SSB}(t) = \cos\left[(\omega_n + \omega_m)t + \frac{\omega_n + \omega_m}{\omega_p}\theta(t)\right]. \qquad (2.11)$$

For the DSB case, the recorder output will be given by

$$e^r_{DSB}(t) = \cos\left[(\omega_n + \omega_m)t + \frac{\omega_n + \omega_m}{\omega_p}\theta(t)\right] + \cos\left[(\omega_n - \omega_m)t + \frac{\omega_n - \omega_m}{\omega_p}\theta(t)\right]. \qquad (2.12)$$

Equations (2.11) and (2.12) indicate that an appropriate model for the tape recorder is a phase modulator, having a modulation input proportional to the recorded frequency. Replacing the tape recorder by a phase modulator yields the model illustrated in Figure 2-2, which is specialized for SSB. In order to analyze a DSB system, the model for the SSB system will be applied first for upper sideband and then for lower sideband. The results of these analyses can be combined to yield the DSB result.

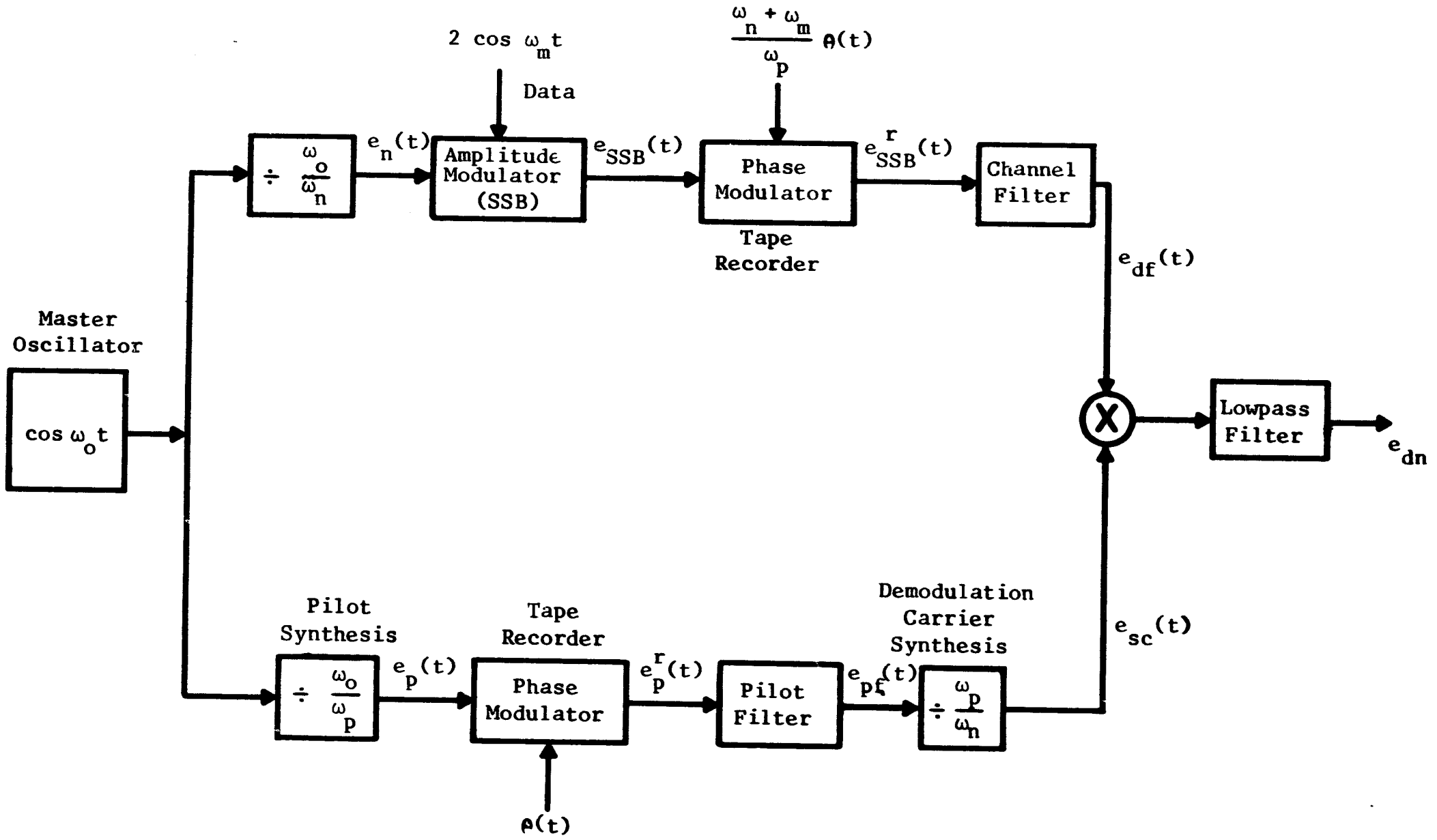

Figure 2-2 System Model with Tape Recorder

III. EFFECT OF FLUTTER ON AN SSB SYSTEM

The model illustrated in Figure 2-2 will now be utilized to determine the effect of recorder flutter on an SSB system. Sinusoidal modulation will be assumed. First, the analysis will be performed neglecting the data and pilot filters, and then the more general problem including filter effects will be investigated.

A. Analysis Neglecting the Data and Pilot Filters

For sinusoidal, single-tone modulation an expression for the SSB signal is

$$e_{SSB}(t) = \cos\ (\omega_n + \omega_m)\, t\ , \tag{3.1}$$

where

ω_n = Channel N carrier frequency, and

ω_m = modulating frequency.

After recording, this signal becomes

$$e^r_{SSB}(t) = \cos\left[(\omega_n + \omega_m)\, t + \frac{\omega_n + \omega_m}{\omega_p}\,\theta(t)\right], \tag{3.2}$$

where

$\theta(t)$ = phase perturbation of the pilot due to flutter, and

ω_p = pilot frequency.

The expression for the synthesized carrier may be derived with the aid of Figure 2-2. The pilot, $e_p(t)$, is

$$e_p(t) = \cos \omega_p t, \tag{3.3}$$

which becomes

$$e_p^r(t) = \cos\left[\omega_p t \quad (+)\right] \tag{3.4}$$

after recording. Since the effect of the pilot filter is being neglected, the synthesized demodulation carrier, $e_{sc}(t)$, becomes

$$e_{sc}(t) = \cos \frac{\omega_n}{\omega_p}\left[\omega_p t + \theta(t)\right] \tag{3.5}$$

or

$$e_{sc}(t) = \cos\left[\omega_n t + \frac{\omega_n}{\omega_p}\theta(t)\right]. \tag{3.6}$$

The demodulated output is then obtained by multiplying together (3.2) and (3.5) and filtering out the $2\omega_n$ term to yield

$$e_{dn}(t) = \frac{1}{2}\cos\left[\omega_m t + \frac{\omega_m}{\omega_p}\theta(t)\right]. \tag{3.7}$$

From (3.7) it is observed that the effect of the recorder is to introduce a phase error proportional to the modulating frequency. There is no interaction between the modulation process and the recorder, since (3.7) would be unchanged if the modulating signal were directly recorded and played back. Thus, this error results when the synthesized demodulation carrier perfectly tracks the carrier position in the data channel. Reducing or compensating for the TBE of the recording system is the only method of eliminating this distortion.

B. Analysis with the Filters

A more complete analysis of the system requires that the effect of the bandpass channel and pilot filters be considered, which involves determining the response of a linear network to a phase-modulated signal. A first order approximation of the filter output may be obtained by utilizing the steady-state transfer function of the filter evaluated at

the instantaneous input frequency, ω_i. This technique is known as the quasi-steady-state approximation[2] and is developed in Appendix C.

The steady-state transfer function of the channel filter may be written in the form

$$H_n(\omega) = \left| H_n(\omega) \right| e^{j\phi(\omega)} , \tag{3.8}$$

where $\left| H_n(\omega) \right|$ and $\phi(\omega)$ represent the amplitude and phase response, respectively. Since the analysis is primarily concerned with the effects of phase, the assumption will be made that the filter has unit amplitude response in the region of interest. The phase response will be assumed linear as in Figure 3-1, so that

$$\phi(\omega) = S_n(\omega - \omega_n) + \theta_n , \tag{3.9}$$

where

S_n = slope of the channel filter phase characteristic, and

θ_n = phase shift of the filter at a frequency ω_n.

Thus, the channel filter transfer function is given by

$$H_n(\omega) = \exp \left[S_n(\omega - \omega_n) + \theta_n \right] . \tag{3.10}$$

If the network is excited by a sinusoid of variable frequency such as

$$e_{in}(t) = \cos \left[\omega_n t + \mu(t) \right] , \tag{3.11}$$

which can be written as

$$e_{in}(t) = \text{Re} \exp j \left[\omega_n t + \mu(t) \right] , \tag{3.12}$$

the quasi-steady-state approximation of the output is

$$e_{out}(t) = \text{Re} \left[H(\omega_i) \exp j \left[\omega_n t + \mu(t) \right] \right] , \tag{3.13}$$

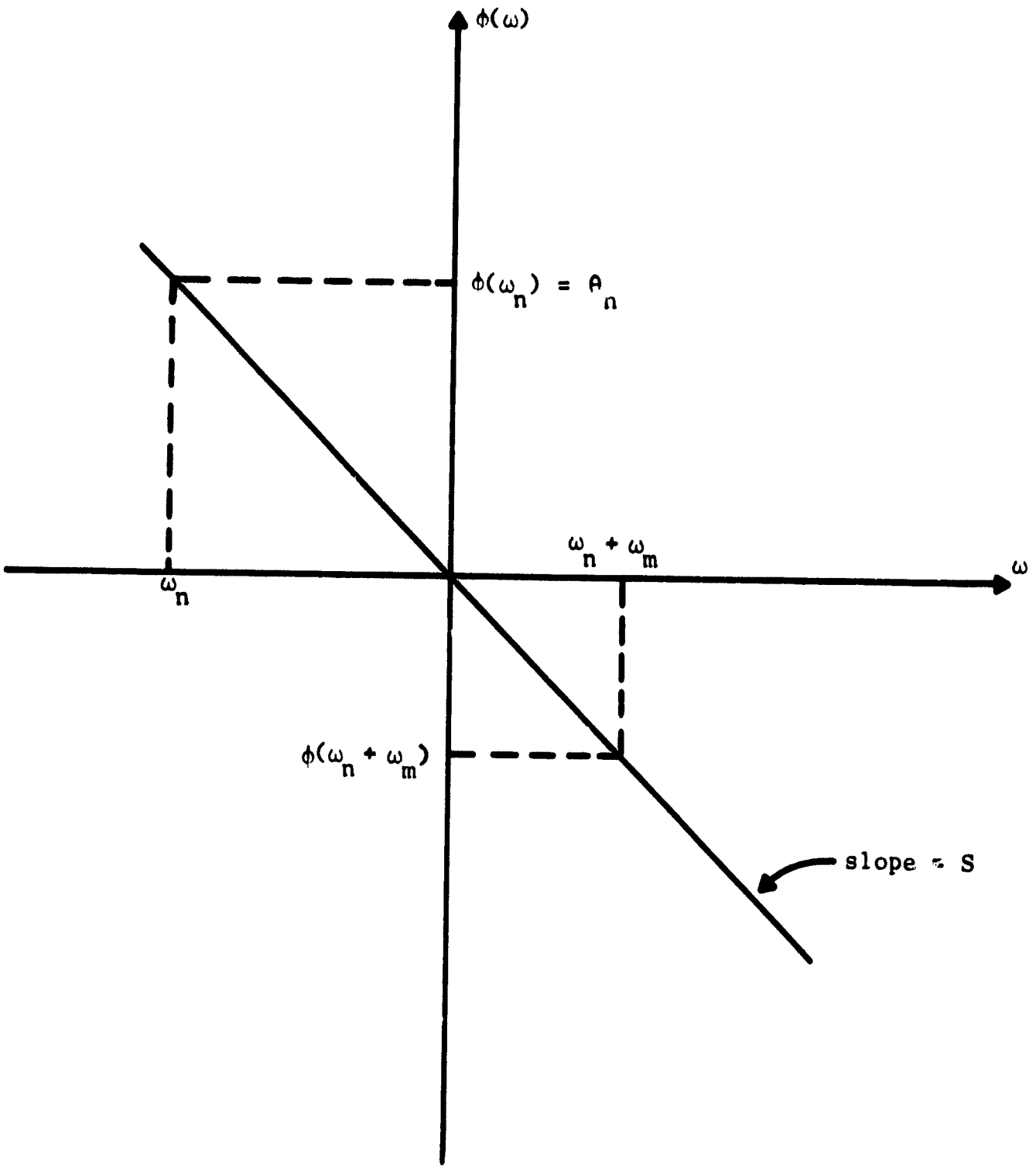

Figure 3-1 Channel-Filter Phase Characteristics Used in SSB Model

where

$$\omega_i = \omega_n + \dot{\mu}(t) \ . \tag{3.14}$$

Substitution of (3.14) into (3.10) yields

$$H_n(\omega_i) = H_n\left[\omega_n + \dot{\mu}(t)\right] = \exp\, j\left[S_n\dot{\mu}(t) + \theta_n\right], \tag{3.15}$$

and (3.13) becomes

$$e_{out}(t) = \mathrm{Re}\, \exp\, j\left[\omega_n t + \mu(t) + S_n\dot{\mu}(t) + \theta_n\right] \ , \tag{3.16}$$

or

$$e_{out}(t) = \cos\left[\omega_n t + \mu(t) + S_n\dot{\mu}(t) + \theta_n\right] \ . \tag{3.17}$$

Note that $\mu(t)$ is the instantaneous phase deviation of the input from the instantaneous channel carrier phase $\omega_n t$, and $\dot{\mu}(t)$, the time derivative of $\mu(t)$, is the instantaneous frequency deviation of the input from the channel carrier frequency, ω_n.

From (3.2) the input to the channel filter is given by

$$e_{SSB}(t) = \cos\left[(\omega_n + \omega_m)t + \frac{\omega_n + \omega_m}{\omega_p}\,\theta(t)\right] \ . \tag{3.18}$$

Inspection of this equation yields

$$\mu(t) = \omega_m t + \frac{\omega_n + \omega_m}{\omega_p}\,\theta(t) \ , \tag{3.19}$$

and

$$\dot{\mu}(t) = \omega_m + \frac{\omega_n + \omega_m}{\omega_p}\,\dot{\theta}(t) \ . \tag{3.20}$$

Substitution of these values into (3.17) yields

$$e_{df}(t) = \cos\left[\omega_n t + \omega_m t + \frac{\omega_n + \omega_m}{\omega_p}\theta(t) + S_n\omega_m + S_n\frac{\omega_n + \omega_m}{\omega_p}\dot{\theta}(t) + \theta_n\right] \tag{3.21}$$

as the channel filter output for the SSB system.

The pilot filter output may be found in exactly the same manner, or it may be determined from (3.21) by setting ω_m and θ_n equal to zero and setting ω_n equal to ω_p. The term ω_m is zero since there is no data modulation on the pilot, and θ_n is zero because the pilot is assumed centered in the pilot filter, i.e., the phase shift is assumed zero at the frequency ω_p. Therefore, the output of the pilot filter is given by

$$e_{pf}(t) = \cos\left[\omega_p t + \theta(t) + S_p\dot{\theta}(t)\right] , \tag{3.22}$$

where S_p represents the slope of the phase characteristic of the pilot filter. The output of the divide by ω_p/ω_n network is the synthesized demodulation carrier, which is

$$e_{sc}(t) = \cos\left[\omega_n t + \frac{\omega_n}{\omega_p}\theta(t) + S_p\frac{\omega_n}{\omega_p}\dot{\theta}(t)\right] . \tag{3.23}$$

The Channel N demodulated output, $e_{dn}(t)$, may now be found by multiplying (3.21) and (3.23) together and filtering out the $2\omega_n$ component. The result is

$$e_{dn}(t) = \frac{1}{2}\cos\left[\omega_m t + \frac{\omega_m}{\omega_p}\theta(t) + S_n\omega_m + (S_n - S_p)\frac{\omega_n}{\omega_p}\dot{\theta}(t) + S_n\frac{\omega_m}{\omega_p}\dot{\theta}(t) + \theta_n\right] , \tag{3.24}$$

which becomes

$$\underset{(A)}{} \quad \underset{(B)}{} \quad \underset{(C)}{} \quad \underset{(D)}{} \quad \underset{(E)}{}$$

$$e_{dn}(t) = \frac{1}{2} \cos \left[\omega_m t + \theta_n + S_n \omega_m + \frac{\omega_m}{\omega_p} \theta(t) + \frac{\omega_m}{\omega_p} S_n \dot{\theta}(t) \right] \qquad (3.25)$$

if the phase slopes of the linear-phase filters are equal. This condition essentially requires that the time-delay through the data channel and the pilot channel be equal. Term (A) is the desired term since the modulating signal was cos $\omega_m t$. Terms (B) and (C) do not cause distortion, since (B) can be eliminated by passing the pilot through a constant-phase-shift network and(C)is a phase shift proportional to frequency, i.e., a constant time-delay. Term (D) represents the distortion term which results from flutter without consideration of the filters, i.e., the distortion term in (3.7), and finally, term (E) represents distortion caused by the interaction of the flutter perturbation with the data filter. Therefore, the effect of flutter on an SSB system can be reduced to the two distortion terms (D) and (E) if the proper linear-phase filters are used and if a constant phase-shift network is used to compensate for the carrier frequency not being centered in the data filter passband.

Data taken from several older recorders allow the relative magnitudes of the distortion terms in (3.25) to be approximated. A typical system would have a maximum modulating frequency of 3 kHz and a pilot frequency of 76 kHz. The slope of the phase characteristics of typical filters would be approximately 10^{-4}s. The recorder data taken indicated that instantaneous phase deviation of a 76 kHz signal can be as large as three radians, and instantaneous frequency deviations can be as large as 150 Hz. These values yield

$$\text{Max} \left[\frac{\omega_m}{\omega_p} \theta(t) \right] = 0.12 \text{ rad}$$

and

$$\text{Max}\left[S_n \frac{\omega_m}{\omega_p} \dot{\alpha}(t)\right] = 0.0037 \text{ rad.}$$

From these expressions, it is clear that Term (D) is usually of more importance and that it may introduce significant error.

IV. EFFECT OF FLUTTER ON A DSB SYSTEM

The model in Figure 2-2 can be used to analyze a DSB system by applying the principle of superposition to the output of an upper and a lower SSB system. From (2.12) the input to the channel filter may be written as

$$e^{r}_{DSB}(t) = \cos\left[(\omega_n + \omega_m)\,t + \frac{\omega_n + \omega_m}{\omega_p}\,\theta(t)\right] + \cos\left[(\omega_n - \omega_m)\,t + \frac{\omega_n - \omega_m}{\omega_p}\,\theta(t)\right], \tag{4.1}$$

where the first term represents the upper sideband and the second term represents the lower sideband. The assumed characteristic for the DSB channel filter is illustrated in Figure 4-1 and can be expressed as

$$\phi(\omega) = S_n(\omega - \omega_n)\ , \tag{4.2}$$

which is (3.9) with θ_n equal to zero since the DSB channel carrier is assumed centered in the filter passband. Thus the channel filter output is given by

$$e_{out}(t) = \cos\left[\omega_n t + \mu(t) + S_n\dot{\mu}(t)\right]\ , \tag{4.3}$$

which is (3.17) with θ_n equal to zero. This output was derived for an input given by

$$e_{in}(t) = \cos\left[\omega_n t + \mu(t)\right]\ . \tag{4.4}$$

For the upper sideband the instantaneous phase deviation is given by

$$\mu(t) = \omega_m t + \frac{\omega_n + \omega_m}{\omega_p}\,\theta(t)\ , \tag{4.5}$$

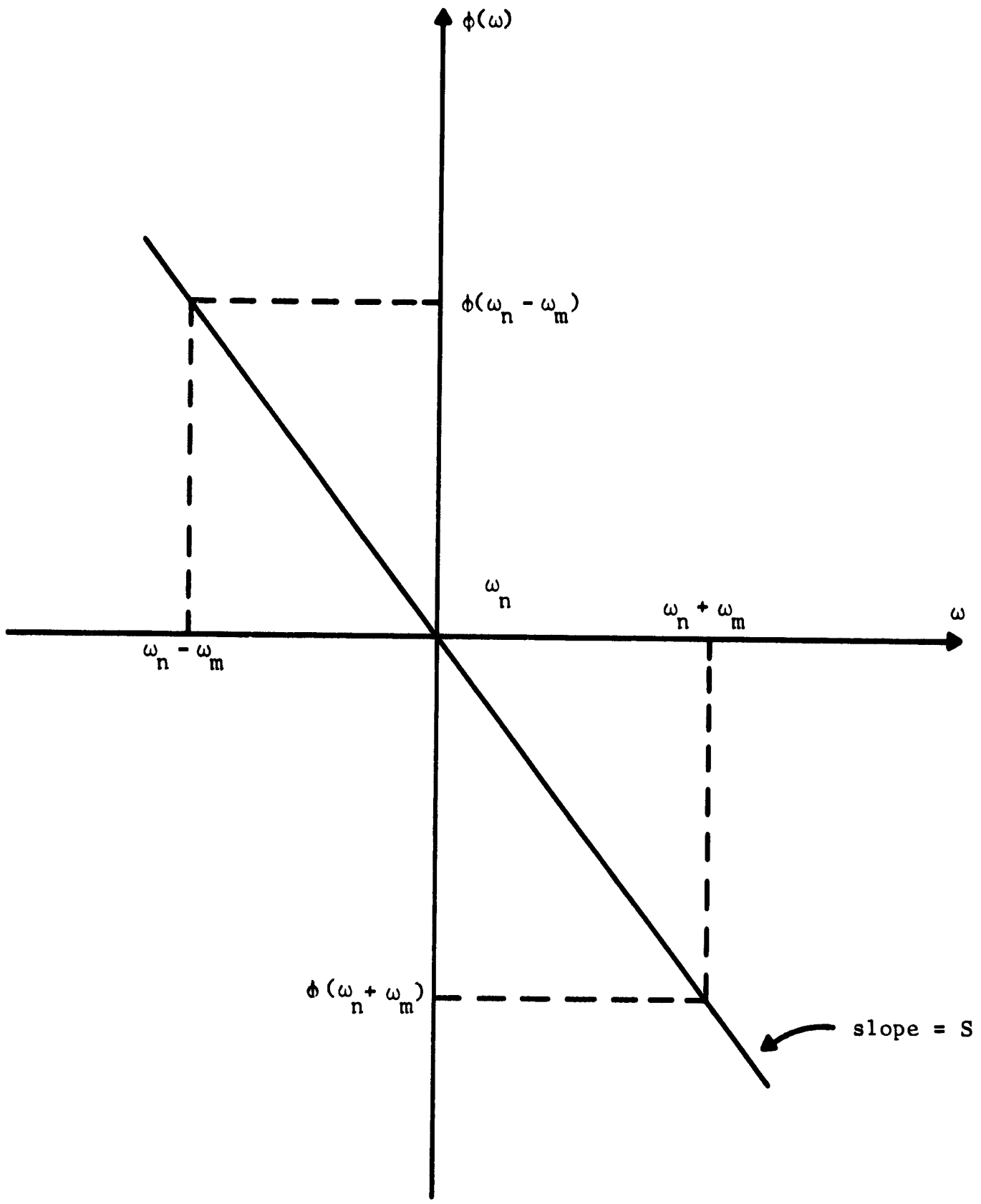

Figure 4-1 Channel-Filter Phase Characteristics Used in DSB Model

and thus, the frequency deviation is given by

$$\dot{\mu}(t) = \omega_m + \frac{\omega_n + \omega_m}{\omega_p} \dot{\theta}(t) \ . \tag{4.6}$$

From (4.1) the upper sideband output, $e_U(t)$, is given by

$$e_U(t) = \cos \left[(\omega_n + \omega_m) t + \frac{\omega_n + \omega_m}{\omega_p} \theta(t) + S_n \omega_m \right.$$
$$\left. + S_n \frac{\omega_n + \omega_m}{\omega_p} \dot{\theta}(t) \right] , \tag{4.7}$$

which is (3.21) with θ_n equal to zero. For the lower sideband the instantaneous phase deviation is given by

$$\mu(t) = -\omega_m t + \frac{\omega_n - \omega_m}{\omega_p} \theta(t), \tag{4.8}$$

and the frequency deviation is given by

$$\dot{\mu}(t) = -\omega_m + \frac{\omega_n - \omega_m}{\omega_p} \dot{\theta}(t). \tag{4.9}$$

The lower sideband output, $e_L(t)$, may now be found using (4.1). The result is

$$e_L(t) = \cos \left[(\omega_n - \omega_m) t + \frac{\omega_n - \omega_m}{\omega_p} \theta(t) - S_n \omega_m + S_n \frac{\omega_n - \omega_m}{\omega_p} \dot{\theta}(t) \right] . \tag{4.10}$$

The total channel filter output for the DSB case is then found by

summing (4.7) and (4.10) to yield

$$e_{df}(t) = \cos\left[(\omega_n + \omega_m)\,t + \frac{\omega_n + \omega_m}{\omega_p}\,\theta(t) + S_n\omega_m + S_n\,\frac{\omega_n + \omega_m}{\omega_p}\,\dot{\theta}(t)\right]$$

$$+ \cos\left[(\omega_n - \omega_m)\,t + \frac{\omega_n - \omega_m}{\omega_p}\,\theta(t) - S_n\omega_m + S_n\,\frac{\omega_n - \omega_m}{\omega_p}\,\dot{\theta}(t)\right]. \tag{4.11}$$

The synthesized demodulation carrier is the same for DSB as for SSB and is given by (3.23). Multiplication of (4.11) and (3.23) and filtering out the $2\omega_n$ terms yield

$$e_{dn}(t) = \frac{1}{2}\cos\left[\omega_m t + \frac{\omega_m}{\omega_p}\,\theta(t) + S_n\omega_m + (S_n - S_p)\,\frac{\omega_n}{\omega_p}\,\dot{\theta}(t) + S_n\,\frac{\omega_m}{\omega_p}\,\dot{\theta}(t)\right]$$

$$+ \frac{1}{2}\cos\left[-\omega_m t - \frac{\omega_m}{\omega_p}\,\theta(t) - S_n\omega_m + (S_n - S_p)\,\frac{\omega_n}{\omega_p}\,\dot{\theta}(t) - S_n\,\frac{\omega_m}{\omega_p}\,\dot{\theta}(t)\right] \tag{4.12}$$

for the demodulated output. If $S_n = S_p$, the sidebands add coherently in the demodulation process and (4.10) becomes

$$e_{dn}(t) = \cos\left[\omega_m t + S_n\omega_m + \frac{\omega_m}{\omega_p}\,\theta(t) + S_n\,\frac{\omega_m}{\omega_p}\,\dot{\theta}(t)\right], \tag{4.13}$$

which is identical with the result obtained for SSB except for the θ_n term does not appear. Thus, assuming that the synthesized demodulation carrier perfectly tracks the channel carrier position, the distortion in $e_{dn}(t)$ is the same for both SSB and DSB modulation. It is important to note that if S_n does not equal S_p, coherent addition of the sidebands does not occur, and additional distortion results.

V. EFFECT OF PILOT NOISE

In the previous chapters the performance of the system is analyzed for the case where the baseband spectrum is perturbed by tape recorder flutter. The assumption was made that the recorder flutter was the only deteriorating effect in the system. The following analysis will assume that flutter is zero and that the pilot is subjected to additive noise, which, by virture of the pilot filter, is narrow-band. The effect of this noise will be to impart a phase perturbation to the pilot, which will lead to a dynamic phase error in the synthesized demodulation carrier. The magnitude of this phase perturbation will be determined as a function of the pilot signal-to-noise ratio.

The analysis which follows will be general and the results specialized to a meaningful form. The work of Rice[3], Hancock[4], and Panter[5] will be closely followed.

In Appendix D, the represention of narrow-band noise about a frequency ω_c is given as

$$n(t) = X(t) \cos \omega_c t + Y(t) \sin \omega_c t, \tag{5.1}$$

where X(t) and Y(t) are statistically independent gaussian processes with zero means and equal variances. The signal which this noise acts upon will have an assumed frequency, ω_p, the center frequency of the pilot filter, and may be written as

$$s(t) = E_p \cos \left[\omega_p t - \phi_p \right] \tag{5.2}$$

or

$$s(t) = a \cos \omega_p t + b \sin \omega_p t, \tag{5.3}$$

where

$$E_p = \sqrt{a^2 + b^2}\ , \tag{5.4}$$

and

$$\phi_p = \tan^{-1} \frac{b}{a} . \tag{5.5}$$

Thus, the output of the pilot filter is the sum of the signal and narrow-band noise and may be written (for $\omega_c = \omega_p$) as

$$e(t) = s(t) + n(t) = \left[a + X(t)\right] \cos \omega_p t + \left[b + Y(t)\right] \sin \omega_p t, \tag{5.6}$$

or

$$e(t) = R(t) \cos\left[\omega_p t + \phi(t)\right] . \tag{5.7}$$

The envelope, R(t), is given by

$$R(t) = \sqrt{\left[a + X(t)\right]^2 + \left[b + Y(t)\right]^2} \tag{5.8}$$

and the phase is

$$\phi(t) = \tan^{-1} \frac{b + Y(t)}{a + X(t)} . \tag{5.9}$$

In order to determine the effect of the noise upon the pilot phase, a density function is needed for $\phi(t)$. To obtain this function the joint density function $q(r,\phi)$ will be determined, and from this density function, $q(\phi)$ will be determined by integration over all r. The joint density function may be found by defining the random variables $X_1(t)$ and $Y_1(t)$ as

$$X_1(t) = a + X(t), \tag{5.10}$$

and

$$Y_1(t) = b + Y(t). \tag{5.11}$$

Since X(t) and Y(t) are gaussian random variables with zero means, $X_1(t)$ and $Y_1(t)$ will be gaussian random varibles with means a and b, respectively. Thus, the density functions, $p(x_1)$ and $p(\,\,$ may be written as

$$p(x_1) = \frac{1}{\sqrt{2\pi}\,\sigma} \; e^{-(y_1 - b)^2/2\sigma^2} \,, \tag{5.12}$$

and

$$p(y_1) = \frac{1}{\sqrt{2\pi}\,\sigma} \; e^{-(y_1 - b)^2/2\sigma^2} \,. \tag{5.13}$$

Since X(t) and Y(t) are statistically independent, $X_1(t)$ and $Y_1(t)$ are also statistically independent. The joint function, $p(x_1,y_1)$, is therefore given by

$$p(x_1,y_1) = p(x_1)\; p(y_1) \tag{5.14}$$

or

$$p(x_1,y_1) = \frac{1}{2\pi\sigma^2} \; e^{-\left[(x_1 - a)^2 + (y_1 - b)^2\right]/2\sigma^2} \,. \tag{5.15}$$

This density function may be transformed into the desired density function, $q(r,\phi)$, by making a change of variables. Let

$$\begin{aligned} r &= x_1^{\,2} + y_1^{\,2}, \\ x_1 &= r\cos\phi, \text{ and} \\ y_1 &= r\sin\phi. \end{aligned} \tag{5.16}$$

Equating probabilities yields

$$p(x_1,y_1)\; dx_1 dy_1 = q(r,\phi)\; dr\, d\phi \,. \tag{5.17}$$

The differential area, $dx_1 dy_1$, transforms into

$$q(r,\phi) = r\, p(x_1, y_1) \,. \tag{5.18}$$

Making the substitutions given by (5.16) into (5.15) yields

$$q(r,\phi) = \frac{r}{2\pi\sigma^2}\, e^{-\left[(r\cos\phi - a)^2 + (r\sin\phi - b)^2\right]/2\sigma^2} \,, \tag{5.19}$$

or

$$q(r,\phi) = \frac{r}{2\pi\sigma^2}\, e^{-\left[r^2 + a^2 + b^2 - 2ar\cos\phi - 2br\sin\phi\right]/2\sigma^2} \,. \tag{5.20}$$

Using (5.20), the density functions $q(r)$ and $q(\phi)$ can be determined. The variations in the envelope of the pilot will be neglected since they can be removed by a limiting process; therefore, $q(r)$ is of no interest. The density function $q(\phi)$ must be examined since it gives the amount of phase perturbation of the pilot due to the noise, and a pilot phase perturbation leads directly to an error in demodulation.

The density function, $q(\phi)$, may be obtained by integrating the joint density function $q(r,\phi)$, over all valves of r. The integration is tedious but straightforward, so it will not be presented here. However, if the substitution

$$z = \frac{E_c^2}{2\sigma^2} = \frac{a^2 + b^2}{2\sigma^2} \tag{5.21}$$

is made, the result for zero reference phase is[6]

$$q(\phi) = \frac{e^{-z}}{2\pi}\left[1 + \sqrt{4\pi z}\,(\cos\phi)\,\Psi\left(\sqrt{2z}\cos\phi\right) e^{z\cos^2\phi}\right], \tag{5.22}$$

where $\Psi(x)$ is the normalized probability integral defined by

$$\Psi(x) = \frac{1}{\sqrt{2\pi}} \int_{-\infty}^{x} e^{-t^2/2}\, dt. \tag{5.23}$$

Equation (5.21) shows that z is the signal-to-noise power ratio. This follows since $E_c^2/2$ is the signal power and the variance, σ^2, is the noise power.

Equation (5.22) is plotted in Figure (5-1) for several values of z. For z equal to zero the density function, $q(\phi)$, is uniform, and as z is increased the density function begins to look gaussian with zero mean. As z continues to increase, the phase perturbations decrease and the density function, $q(\phi)$, approaches a true gaussian function. This can be seen by noting that

$$\Psi(x) \approx 1 - \frac{e^{-x^2/2}}{\sqrt{2\pi}\, x}, \qquad x > 3 . \tag{5.24}$$

Thus, under these conditions

$$\Psi(\sqrt{2z}\cos\phi) \approx 1 - \frac{e^{-z\cos^2\phi}}{2\sqrt{\pi z}\cos\phi}, \tag{5.25}$$

and

$$q(\phi) = \frac{e^{-z}}{2\pi}\left[1 + 2\sqrt{\pi z}\cos\phi\, e^{z\cos^2\phi}\left(1 - \frac{e^{-z\cos^2\phi}}{2\sqrt{\pi z}\cos\phi}\right)\right], \tag{5.26}$$

which becomes

$$q(\phi) \approx \frac{e^{-z}}{2\pi}\left[2\sqrt{\pi z}\cos\phi\, e^{z\cos^2\phi}\right] . \tag{5.27}$$

Equation (5.30) may be written as

$$q(\phi) \approx e^{-z}\sqrt{\frac{z}{\pi}}\cos\phi\, e^{z(1-\sin^2\phi)}, \tag{5.28}$$

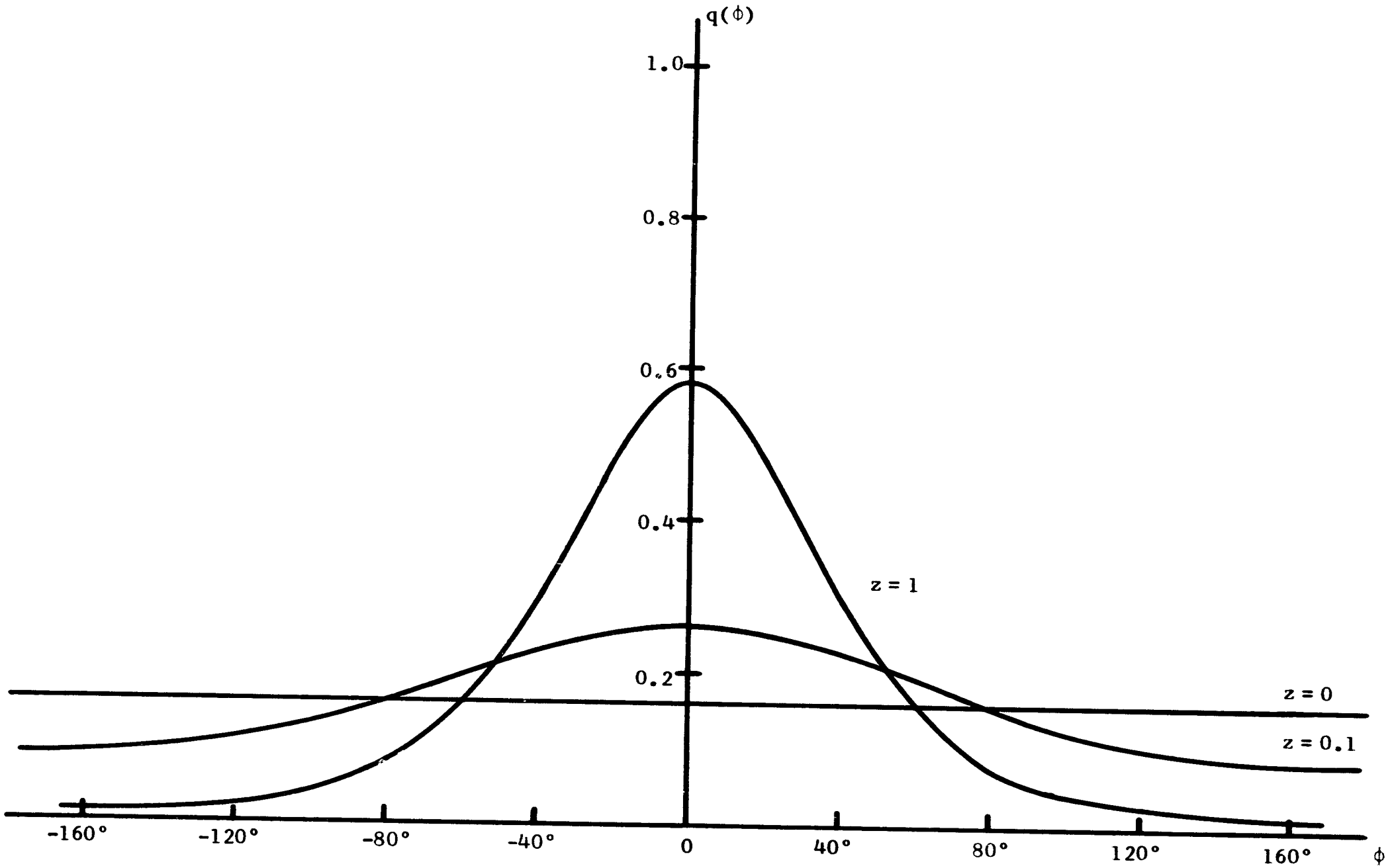

Figure 5-1 Density Function $q(\phi)$ for Small z

or

$$q(\phi) \approx \sqrt{\frac{z}{\pi}} \cos \phi \; e^{-z \sin^2 \phi} \; . \tag{5.29}$$

Equation (5.24) shows that (5.29) is valid where

$$\sqrt{2z} \cos \phi > 3 \; .$$

For large z most of the density function will lie in the region of ϕ equal to zero. Thus, for sufficiently large z, (5.29) can be written as

$$q(\phi) \approx \sqrt{\frac{z}{\pi}} \; e^{-z\phi^2} \; , \tag{5.30}$$

which is a normal distribution with zero mean and variance

$$\sigma_\phi^2 = \frac{1}{2z} \; . \tag{5.31}$$

This expression is useful because the standard deviation,

$$\sigma_\phi = \frac{1}{\sqrt{2z}} \; , \tag{5.32}$$

is the rms phase error.

This phase error, which is plotted in Figure 5-2, is divided for channel carrier frequencies less than the pilot frequency and multiplied for higher carrier frequencies. Thus, phase error in the synthesized demodulation carrier may be more or less than pilot phase error. The effect of these phase errors in investigated in Appendix E for the case of sinusoidal modulation.

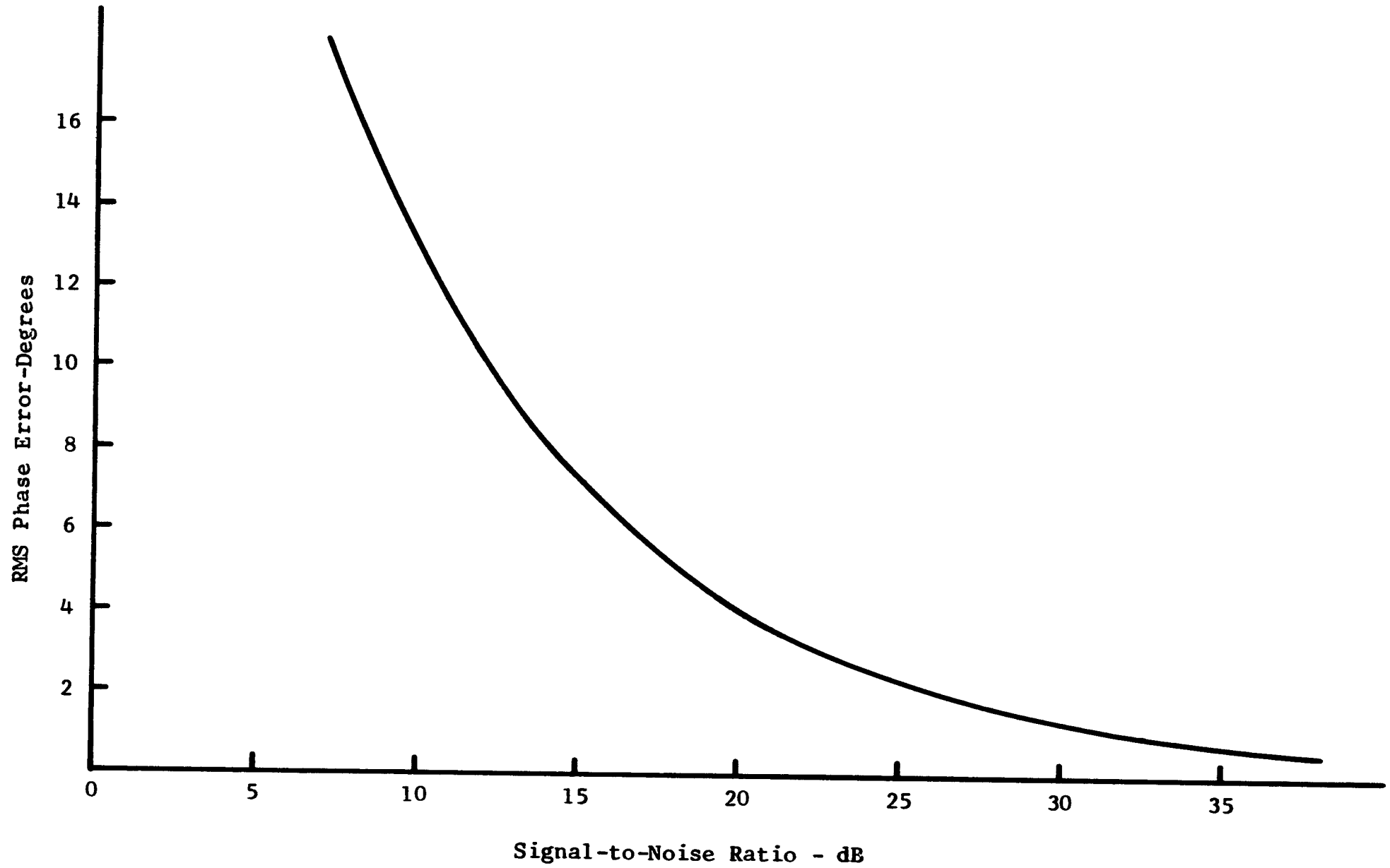

Figure 5-2 RMS Phase Error vs. Signal-to-Noise Ratio

VI. FACTORS AFFECTING PILOT POSITION

There are basically two factors which must be considered before the pilot position in the baseband can be fixed. The first factor results from the triangular noise spectrum which exists on the baseband due to noise in the receiver rf. Consideration of this factor of course indicates that the pilot location should be low in the baseband if the receiver rf noise level is high. This effect is well understood and if the pilot bandwidth and the receiver rf signal-to-noise ratio are known, the maximum pilot frequency can be determined.

Another problem which must be considered is the effect of the pilot position when the baseband is perturbed by tape recorder flutter. When the pilot frequency is low, it must be multiplied in order to synthesize higher frequency demodulation carriers. The resulting situation is illustrated in Figure 6-1, where the synthesized demodulation carrier frequency is four times the pilot frequency. Time t_o is assumed to be the real-time position, i.e., t = 0. All preceeding pilot zero crossings and their corresponding times are known accurately. Thus, the length of the interval

$$I_o = t_o - t_{-1} , \tag{6.1}$$

is known. Since this interval is one half the pilot period it is given by

$$I_o = \frac{1}{2f_p'} = \frac{1}{\left[1 + g(t)\right]f_p} , \tag{6.2}$$

where

f_p' = actual pilot frequency

$g(t)$ = instantaneous flutter, and

f_p = nominal pilot frequency.

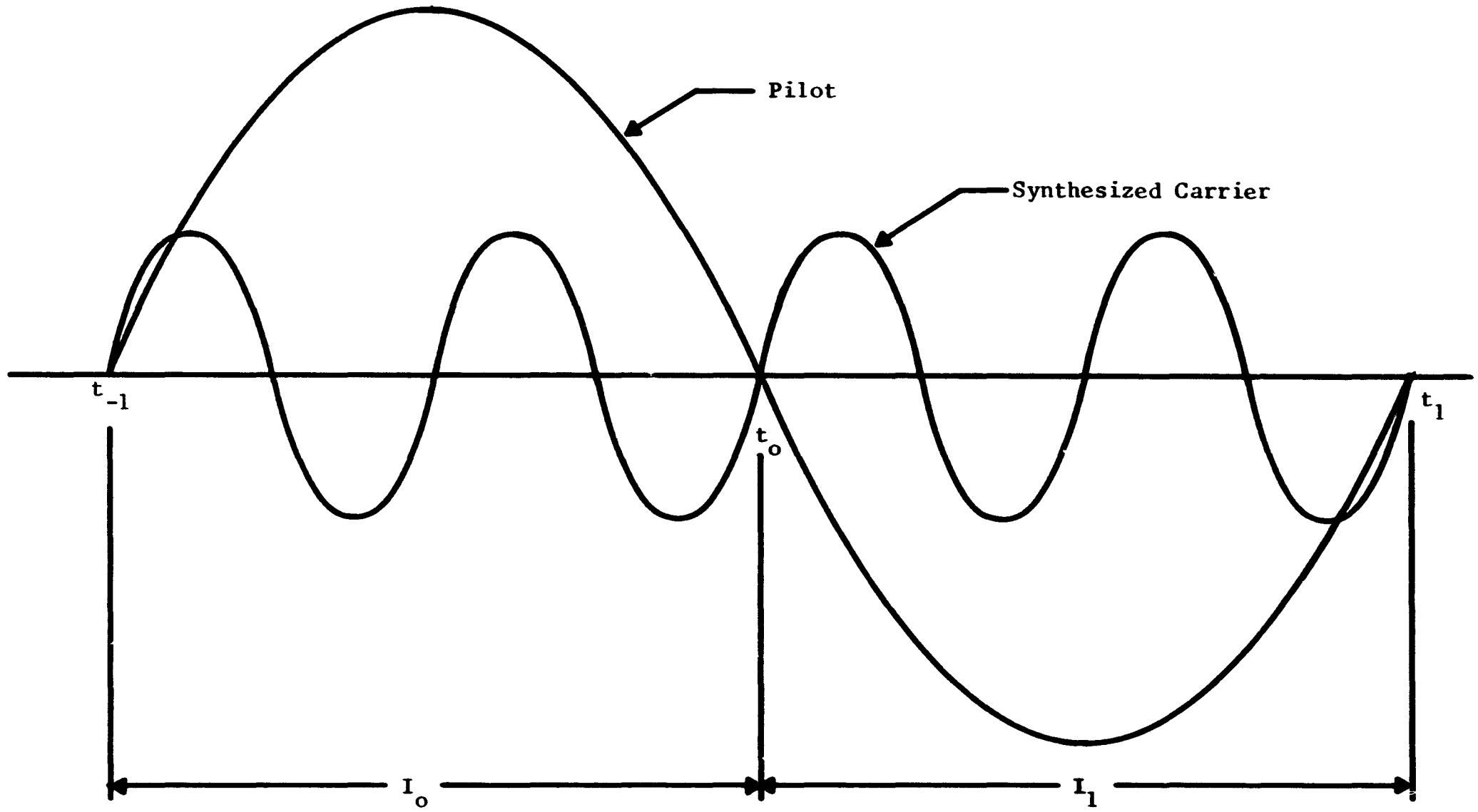

Figure 6-1 Synthesis from a Low-Frequency Pilot

The next pilot zero crossing falls at time t_1, but before the occurrence of this zero crossing, several cycles of the synthesized demodulation carrier occur. Essentially the zero crossings between t_o and t_1 are positioned by assuming that the interval $I_1 = t_1 - t_o$ is equal in length to the interval I_o. The difficulty with this assumption is that TBE, h(t), is a dynamic process and hence changes from interval to interval. Thus, the interval lengths change, and the fact that the zero crossings between t_o and t_1 are placed using "old" information leads to phase errors if a high-frequency carrier is synthesized from a low-frequency pilot. To determine the maximum phase error in the synthesized demodulation carrier, the maximum change in the interval length must be determined. This change, ΔI_m, is given by

$$\Delta I_m = \text{Max} \left[\frac{d}{dt} h(t) \right] I \ , \qquad (6.3)$$

where Max $\left[\frac{d}{dt} h(t) \right]$ represents the maximum time rate of change in TBE and I is the nominal interval length, $\frac{\pi}{\omega_p}$. Since flutter, g(t), is given by

$$g(t) = \frac{d}{dt} h(t), \qquad (6.4)$$

(6.3) may be written as

$$\Delta I_m = \frac{\pi}{\omega_p} g_{max} . \qquad (6.5)$$

where g_{max} is the maximum value of g(t), which is commonly given in recorder specifications.

Equation (6.5) actually gives the maximum time error in predicting the location of the next pilot zero crossing. This time error is transformed into a phase error in the synthesized demodulation carrier by multiplying by the demodulation carrier frequency, ω_n. The resultant

phase error on Channel N, ε_{pn}, is given by

$$\varepsilon_{pn} = \left(\frac{\pi}{\omega_p} g_{max}\right) \omega_n \text{ radians} \tag{6.6}$$

or

$$\varepsilon_{pn} = g_{max} \left(\frac{\omega_n}{\omega_p}\right) (180) \text{ degrees.} \tag{6.7}$$

Equation (6.7) illustrates that the peak phase error occurs on the highest frequency channel. It is therefore useful to define a pilot position parameter, X, as

$$X = \frac{\omega_x}{\omega_p}, \tag{6.8}$$

where ω_x is the highest frequency channel in the composite baseband. Figure 6-2 shows ε_{px}, where

$$\varepsilon_{px} = g_{max} X (180) \text{ degrees,} \tag{6.9}$$

plotted as a function of X. Several typical values of g_{max} are used as parameters.

Another point to be considered in the implementation of the system is the synchronization of the various carriers. For example, if the Channel 1 demodulation carrier is to be synchronized from a pilot on Channel N, a phase ambiguity will exist unless it is known which zero crossing of the Channel N pilot corresponds to the positive going zero crossing of the Channel 1 carrier. Complete baseband synchronization exists when all demodulation carriers are passing through zero with positive slope when the Channel 1 carrier is passing through zero with positive slope. Accomplishment of this synchronization requires an additional bit of information which may be acquired by several techniques. If the pilot is located below all of the carriers, the ambiguity does not exist.

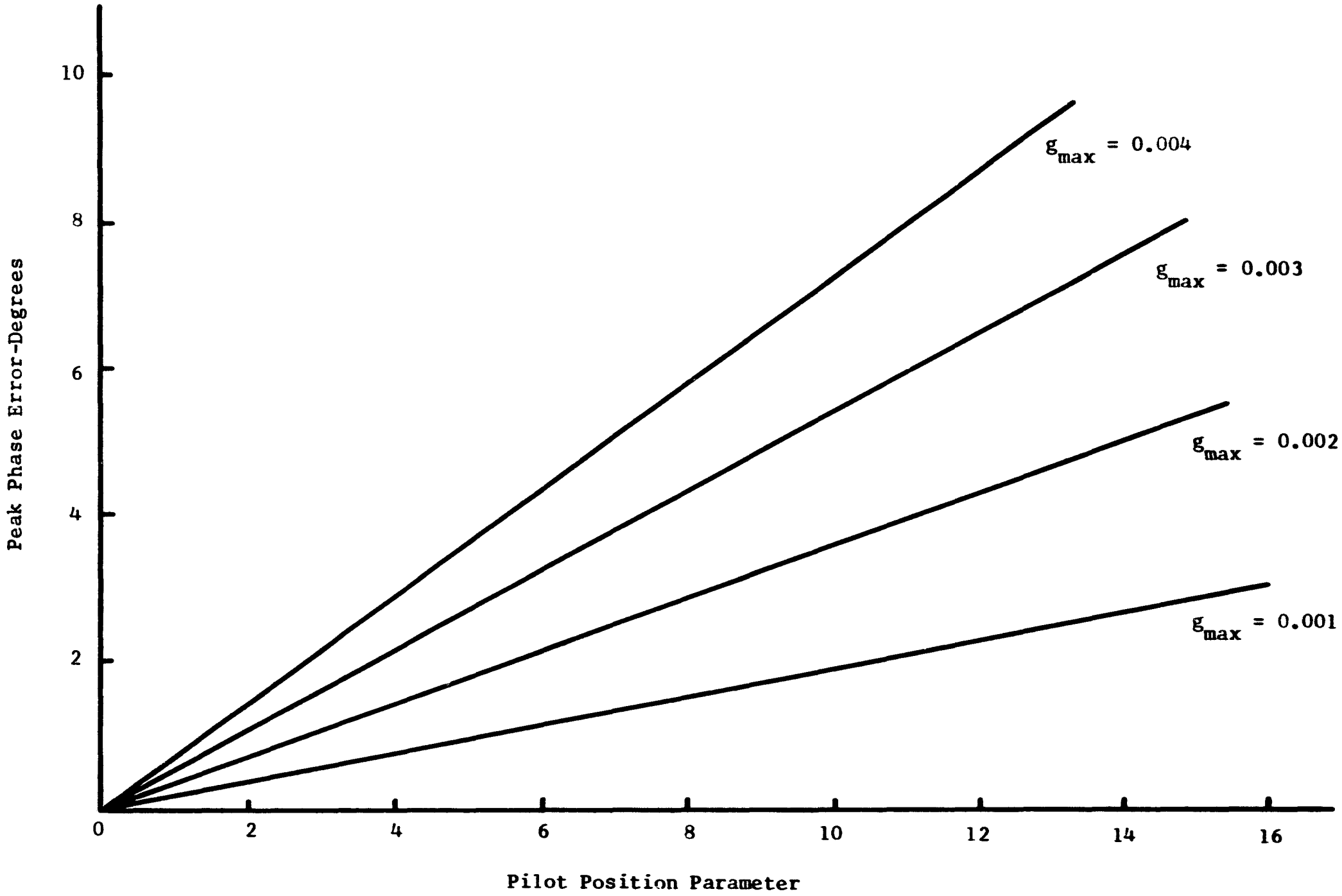

Figure 6-2 Phase Error as a Function of Pilot Position

VII. SUMMARY

The results of the analysis show that if the synthesized demodulation carrier perfectly tracks the carrier position in the channel, an error due to recorder flutter occurs in both SSB and DSB systems. The error is identical in both systems. The error can be decreased either by using recorders having less flutter or by employing a scheme for TBE compensation. Also, the effect of noise on the pilot has been analyzed, and the resulting errors in the demodulated output determined for both SSB and DSB systems. In Appendix E it is shown that these errors are more severe in SSB than in DSB.

In the SSB system a phase correction is needed to compensate for the phase, θ_n, imparted to the channel carrier. For the DSB case the channel carrier is assumed centered in the data channel filter resulting in no phase shift of the carrier. Therefore, the only difference in the ground station implementation of the two systems is a phase compensation network.

In order to eliminate the distortion terms involving

$$(S_n - S_p),$$

S_n must equal S_p. This is equivalent to stating that the time delay of the data and pilot channels must be matched. It should be noted that this does not say that the channel and pilot filters should be identical, but only that the phase characteristics be matched.

APPENDIX A

FLUTTER AND TIME-BASE ERROR IN TAPE RECORDING

In this appendix the effect of flutter is determined for both direct and FM recording, and the conditions under which the effect of flutter is a simple TBE are investigated.[7]

A. Flutter in Direct Recording

In the recording process the instantaneous flutter, $g_r(t)$, is defined as

$$g_r(t) = \frac{v_r(t) - V_r}{V_r} , \qquad (A.1)$$

where $v_r(t)$ is the instantaneous tape velocity and V_r is the mean tape velocity. From (A.1)

$$v_r(t) = V_r \left[1 + g_r(t) \right] . \qquad (A.2)$$

Distance along the tape, $s(\tau)$, can be obtained by integrating (A.2) to give

$$s(\tau) = V_r \left[\tau + \int_o^\tau g_r(t)\, dt \right] . \qquad (A.3)$$

If time-base error (TBE) is defined as

$$h_r(\tau) = \int_o^\tau g_r(t)\, dt , \qquad (A.4)$$

(A.3) can be written as

$$s(\tau) = V_r \left[\tau + h_r(\tau) \right] . \qquad (A.5)$$

Solving (A.5) for τ gives

$$\tau = \frac{s(\tau)}{V_r} - h_r(\tau) \ . \qquad (A.6)$$

Since the peak value of TBE is typically on the order of a millisecond or less, the second term in (A.6) is usually negligible compared to the first term. Thus τ may be approximated by s/V_r, where s is understood to be a function of τ. Thus,

$$\tau = \frac{s}{V_r} - h_r\left(\frac{s}{V_r}\right) . \qquad (A.7)$$

The record circuit will be assumed to result in a tape flux, $\phi(\tau)$, proportional to the recorded signal, or

$$\phi(\tau) = K_r e_r(\tau), \qquad (A.8)$$

where K_r is a recorder constant having units of Webers per volt. Substituting (A.7) into (A.8) yields

$$\phi(s) = K_r e_r \left[\frac{s}{V_r} - h_r\left(\frac{s}{V_r}\right) \right] , \qquad (A.9)$$

an expression for flux along the tape as a function of distance.

Upon playback, the voltage at the output of the read head, $e_p(t)$, is given by

$$e_p(t) = K_p \frac{d}{dt} \phi(s), \qquad (A.10)$$

where K_p is a recorder constant having units of volt-seconds per Weber. Substituting (A.9) into (A.10) yields

$$e_p(t) = K \frac{de_r(\tau)}{dt} \ , \qquad (A.11)$$

where K is the overall recorder constant, $K_r K_p$ and τ is related to s by (A.7). Application of the chain rule yields

$$e_p(t) = K \frac{de_r(\tau)}{d\tau} \frac{d\tau}{ds} \frac{ds}{dt} , \qquad (A.12)$$

which, with the use of (A.7) may be evaluated as

$$e_p(t) = \frac{K}{V_r} \frac{ds}{dt} \left[1 - h_r'\left(\frac{s}{V_r}\right)\right] e_r'\left[\frac{s}{V_r} - h_r\left(\frac{s}{V_r}\right)\right] . \qquad (A.13)$$

In analogy to (A.5) the expression relating time and distance along the tape during playback is

$$s(t) = V_p\left[t + h_p(t)\right] , \qquad (A.14)$$

where $h_p(t)$ is the playback TBE and V_p is the mean tape velocity during playback. Substituting (A.14) into (A.13) and letting V_r equal V_p yields

$$e_p(t) = K\left[1 + h_p'(t)\right]\left[1 - h_r'\left[t + h_p(t)\right]\right] \qquad (A.15)$$
$$X\, e_r'\left[t + h_p(t) - h_r\left[t + h_p(t)\right]\right]$$

or

$$e_p(t) = K\left[1 + h_p'(t) - h_r'\left[t + h_p(t)\right] - h_p'(t)\, h_r'\left[t + h_p(t)\right]\right] \qquad (A.16)$$
$$X\, e_r'\left[t + h_p(t) - h_r\left[t + h_p(t)\right]\right] .$$

If an overall TBE is defined as

$$h(t) = h_p(t) - h_r\left[t + h_p(t)\right] , \qquad (A.17)$$

it follows that the overall flutter, g(t), is given by

$$g(t) = \frac{d}{dt} h(t) = h_p'(t) - h_r'\left[t + h_p(t)\right] - h_p'(t)\, h_r'\left[t + h_p(t)\right] . \quad (A.18)$$

Substituting (A.17) and (A.18) into (A.16) yields

$$e_p(t) = K\left[1 + g(t)\right] e_r'\left[t + h(t)\right] , \quad (A.19)$$

which indicates that flutter results in both a perturbed time base and amplitude. However, if the peak flutter is small, (A.19) may be approximated as

$$e_p(t) = K\, e_r'\left[t + h(t)\right] . \quad (A.20)$$

The derivative indicates that the playback signal must be integrated to yield the output signal

$$e_o(t) = K\, e_r\left[t + h(t)\right] , \quad (A.21)$$

which is the recorded signal perturbed by TBE.

B. Flutter in FM Recording

If $e_r(t)$ is assumed to have the form

$$e_r(t) = E_c \sin\left[\omega_c t + \frac{\Delta\omega_c}{E_m}\int_o^t e_m(t)\, dt\right] , \quad (A.22)$$

the playback signal can be obtained using (A.19) to yield

$$e_p(t) = K\, E_c \omega_c \left[1 + g(t)\right]\left[1 + \frac{\Delta\omega}{\omega_c}\,\frac{e_m\left[t + h(t)\right]}{E_m}\right] \quad (A.23)$$

$$\times \cos\left[\omega_c\left[t + h(t)\right] + \frac{\Delta\omega_c}{E_m}\int_o^{t + h(t)} e_m(t)\, dt\right] .$$

Demodulation of the playback signal yields the output signal, $e_o(t)$, corresponding to the input signal, $e_m(t)$. Thus, determining the instantaneous frequency of the argument of the cosine term in (A.23) yields

$$e_o(t) = \frac{K_d \Delta\omega_c}{E_m} \left[e_m \left[t + h(t) \right] + g(t) \left[E_m + e_m \left[t + h(t) \right] \right] \right] , \qquad (A.24)$$

where K_d is a discriminator constant having units of volts per Hertz. If $g(t)$ is small (A.24) may be approximated as

$$e_o(t) = \frac{K_d \Delta\omega_c}{E_m} \; e_m \left[t + h(t) \right] . \qquad (A.25)$$

As for direct recording the effect of flutter in FM recording is a time-base perturbation, provided the flutter is sufficiently small to allow the additive noise term in (A.24) to be ignored.

APPENDIX B

CARRIER SYNTHESIS BY FREQUENCY DIVISION

In Chapter II it was stated that if all channel carriers are harmonically related, they may be synthesized from a master oscillator by dividing the proper master oscillator frequency by an appropriate number. There are many ways by which this may be accomplished. The purpose of this appendix is to illustrate one of these methods in order to make the system model clearer.

For purposes of illustration, assume that the baseband is a 16 channel format with the pilot at Channel 16. The frequency of the Channel 1 carrier is ω_1, and

$$\omega_n = N\omega_1, \tag{B.1}$$

where ω_n is the Channel N carrier frequency. The pilot frequency, ω_p, is given by (B.1) with N equal to 16.

A synthesis scheme is shown in Figure B.1 which allows the Channel 16,15,12,10,8,6,5,4, and 3 carriers to be synthesized directly from a master oscillator running at a frequency of 480 ω_1. The remaining channel carriers may be synthesized by the multiplication technique illustrated where the multipliers are followed by bandpass filters having appropriate center frequencies. The frequency division process is illustrated in Figure B.2 where

$$\sin\left(\omega t + \frac{\pi}{2}\right)$$

is divided by two and by four.

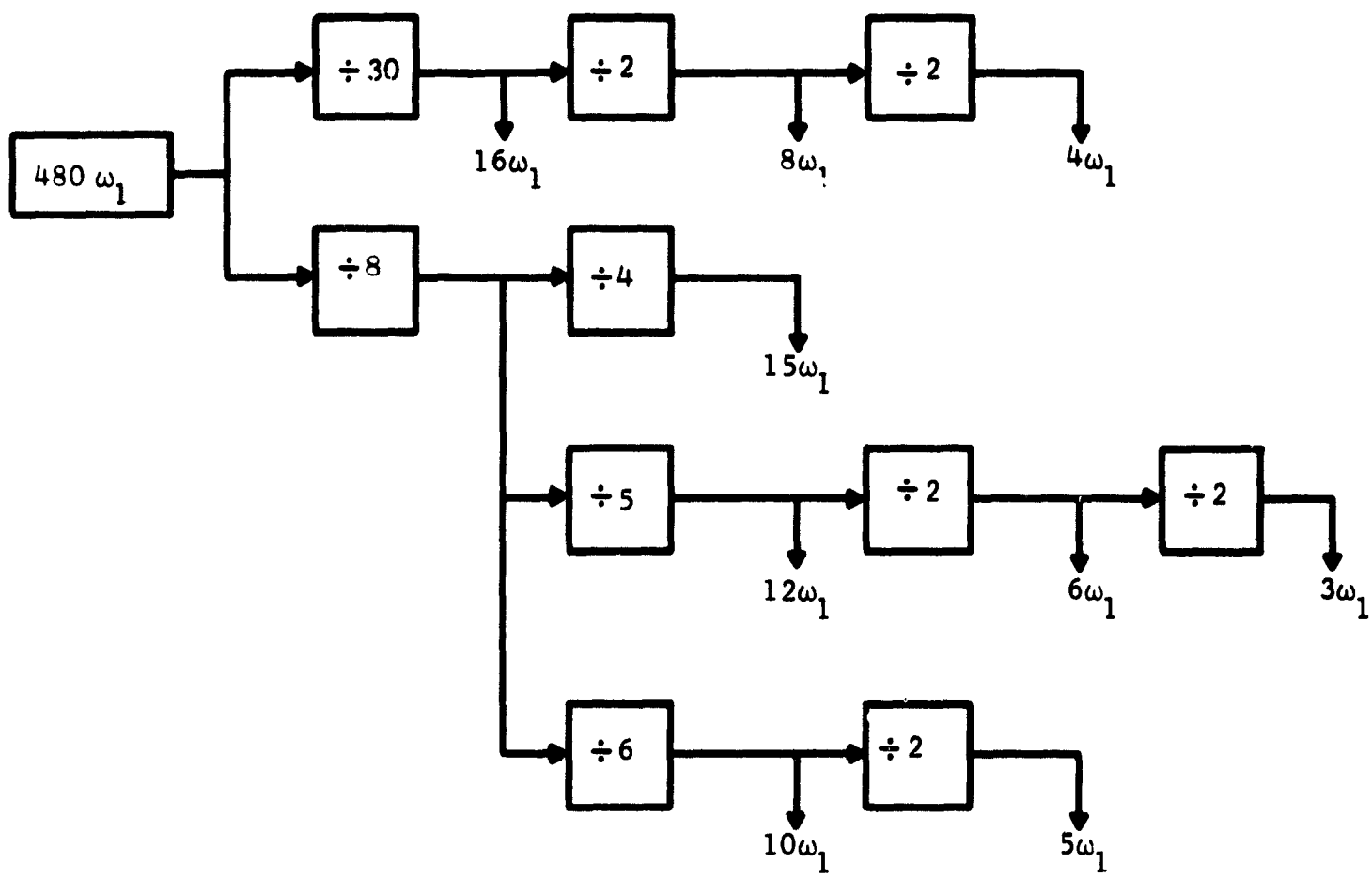

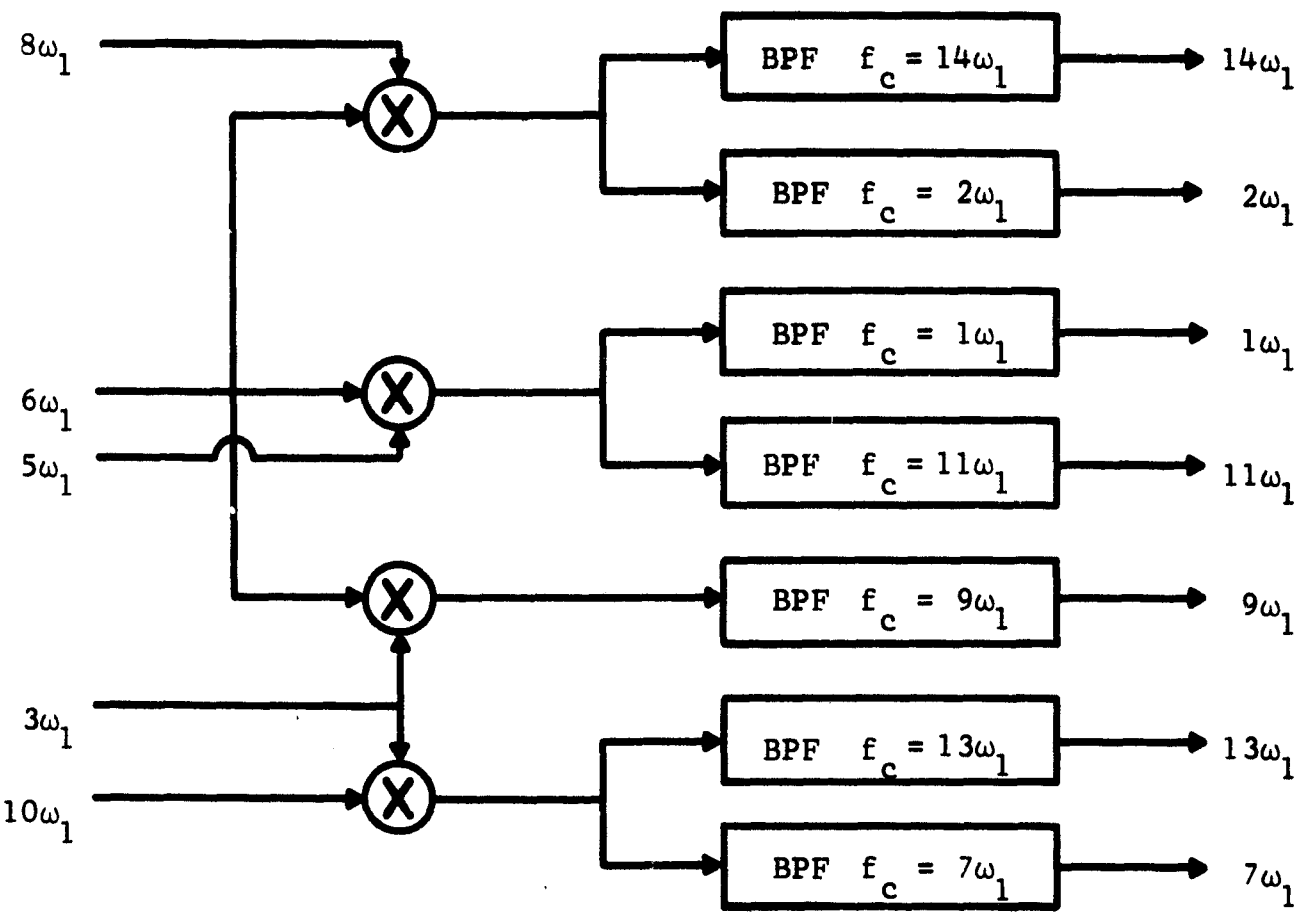

Figure B-1 Carrier Synthesis

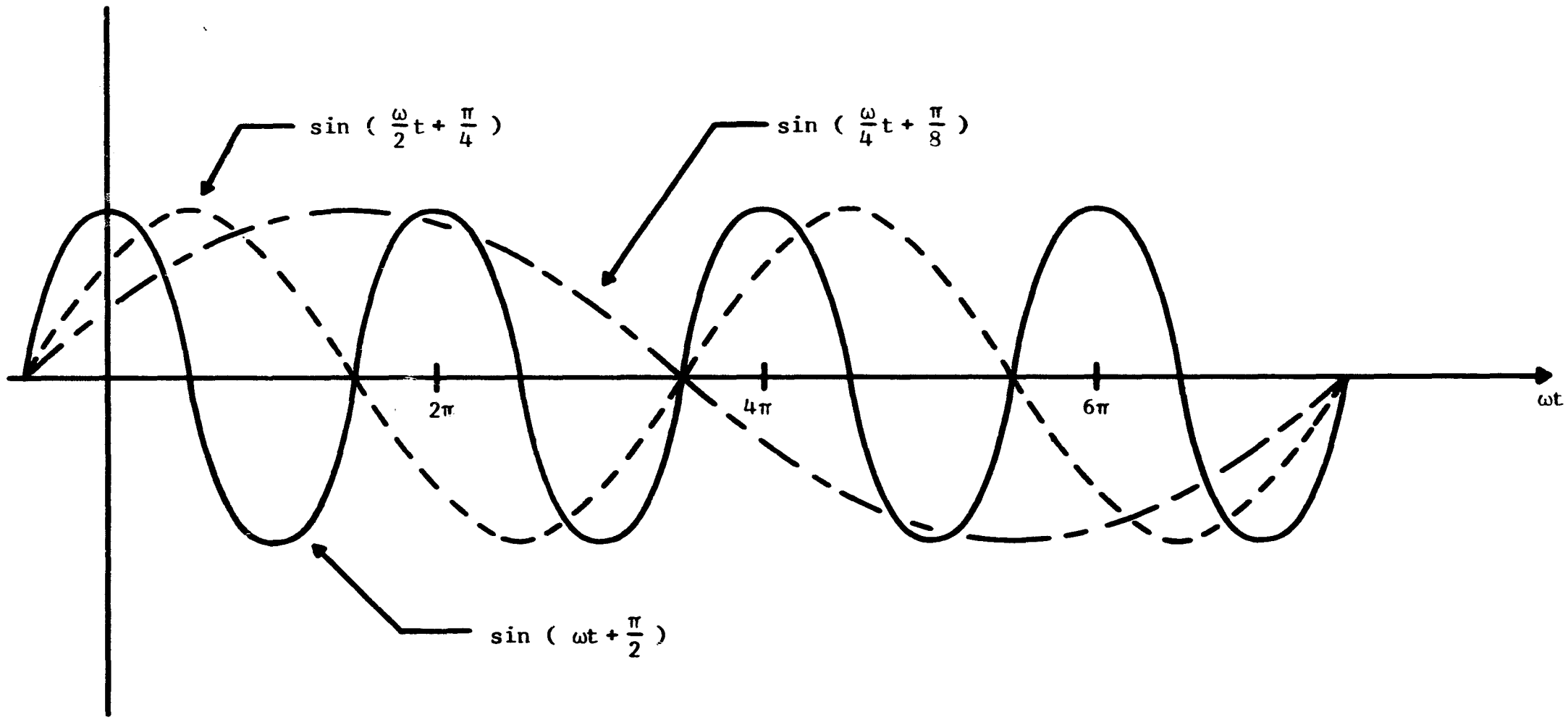

Figure B-2 Illustration of Frequency Division

APPENDIX C

RESPONSE OF A LINEAR NETWORK TO A VARIABLE FREQUENCY INPUT

In analyzing the response of a network to a variable frequency or FM input, there are two approaches which may be used. The first method of analysis requires that the input to the network be expanded into its sinusoidal components. This expansion yields the spectrum of the input and takes the form of a Fourier-Bessel series. The network then selects components in the spectrum and imparts to each component an amplitude scaling and a phase shift. The result of this operation is the spectrum of the output. This method has a disadvantage in that the computations are often long, and the result is a series which usually cannot be written in closed form. Thus, the true form of the response is often obscured by the complexity of the answer. This approach is often called the spectral approach.[8]

The second approach is to consider the network as a dynamic system. There is a limit on the speed at which the response of a frequency selective network can build up or decay. This results from the fact that all frequency selective networks contain energy storage elements. Thus, these networks exhibit an inertia or sluggishness of response, and the network is analyzed on this basis.

The dynamic approach was first investigated by Carson and Fry in their classic paper published in 1937.[9] They show that the response of a network to an FM input can be broken down into two components, the quasi-steady-state component and the distortion component. The quasi-steady-state component represents that part of the response which can be obtained from sinusoidal steady-state network analysis by substituting the variable instantaneous frequency for the assumed constant frequency in the transfer function given by sinusoidal steady-state network theory. If the response of the network can build up or decay very quickly, the quasi-steady-state component approximates closely the total solution. Often however, the system is too sluggish to meet this condition and a correction or distortion

term is needed in addition to the quasi-steady-state term. This correction term usually takes the form of an infinite series.

Several others since Carson and Fry have published papers which bear on this problem. The most notable of these papers are the ones by Van der Pol,[10] Stumpers,[11] and Baghdady.[12]

The response of a network to an FM signal will now be developed. The two terms in the response will be indicated and the condition which must hold for the distortion term to be negligible will be derived. The work presented here follows closely a paper by G. A. Morley.[13]

Consider a network where

$e_i(t)$ = input to the network,

$e_o(t)$ = output of the network,

$h(t)$ = unit impulse response, and

$Y(s)$ = the Laplace transform of $h(t)$.

Let the input to the network be written as

$$e_i(t) = e^{j\theta(t)}, \tag{C.1}$$

or

$$e_i(t) = e^{j\int \omega_i(t)\, dt}, \tag{C.2}$$

where $\omega_i(t)$ represents the instantaneous frequency of the input. The transfer function of the network, $Y(s)$, may be written as

$$Y(s) = \sum_{\alpha} \frac{A_\alpha}{s - s_\alpha}, \tag{C.3}$$

where the s_α's are the poles of the function $Y(s)$. Consistent with (C.3),

the unit impulse response may be written as

$$h(t) = \begin{cases} \sum_{\alpha} A_{\alpha} e^{s_{\alpha} t} & t \geq 0 \\ 0 & t < 0 \end{cases} \qquad (C.4)$$

The output of the network may be obtained by using the convolution integral, or

$$e_o(t) = \int_o^t h(t - \tau)\, e_i(\tau)\, d\tau. \qquad (C.5)$$

Using (C.4), this may be written as

$$e_o(t) = \int_o^t \sum_{\alpha} A_{\alpha} e^{s_{\alpha}(t - \tau)} e_i(\tau)\, d\tau \qquad (C.6)$$

or

$$e_o(t) = \sum_{\alpha} A_{\alpha} e^{s_{\alpha} t} \int_o^t e^{-s_{\alpha}\tau} e_i(\tau)\, d\tau\ . \qquad (C.7)$$

From the above expression, it is clear that $e_o(t)$ may be written as

$$e_o(t) = \sum_{\alpha} e_{\alpha}(t)\ , \qquad (C.8)$$

where

$$e_{\alpha}(t) = A_{\alpha} e^{s_{\alpha} t} \int_o^t e^{-s_{\alpha}\tau} e_i(\tau)\, d\tau\ . \qquad (C.9)$$

Using (C.2) $e_\alpha(t)$ may be written in terms of the instantaneous input frequency as

$$e_\alpha = A_\alpha e^{s_\alpha t} \int_o^t e^{-s_\alpha \tau} \exp\left[j \int \omega_i(\tau)\, d\tau \right] d\tau \,. \qquad (C.10)$$

or

$$e_\alpha = A_\alpha e^{s_\alpha t} \int_o^t \exp\left[-s_\alpha \tau + j \int \omega_i(\tau)\, d\tau \right] d\tau \,. \qquad (C.11)$$

In order to perform the integration indicated in (C.11), it is convenient to introduce a function $\mu(\tau)$, defined as

$$\mu(\tau) = -s_\alpha \tau + j \int \omega_i(\tau)\, d\tau \,. \qquad (C.12)$$

Equation (C.11) then becomes

$$e_\alpha(t) = A_\alpha e^{s_\alpha t} \int_o^t e^{\mu(\tau)}\, d\tau \,, \qquad (C.13)$$

which may be integrated by parts by considering

$$\int_o^t e^{\mu(\tau)}\, d\tau = \int_o^t \frac{e^{\mu(\tau)} \dfrac{d\mu(\tau)}{d\tau}}{\dfrac{d\mu(\tau)}{d\tau}}\, d\tau \qquad (C.14)$$

and by defining

$$v = e^{\mu(\tau)} \,,$$

$$\frac{dv}{d\tau} = e^{\mu(\tau)} \frac{d\mu(\tau)}{d\tau} \,,$$

$$dv = e^{\mu(\tau)} \frac{d\mu(\tau)}{d\tau} d\tau \ ,$$

$$\mu = \frac{1}{\frac{d\mu(\tau)}{d\tau}} \ , \text{ and} \qquad \text{(C.15)}$$

$$\frac{d\mu}{d\tau} = \frac{-\frac{d^2\mu(\tau)}{d\tau^2}}{\left(\frac{d\mu(\tau)}{d\tau}\right)^2} \ .$$

Thus,

$$\int_o^t e^{\mu(\tau)} \, d\tau = \left[\frac{e^{\mu(\tau)}}{\frac{d\mu(\tau)}{d\tau}}\right]_o^t + \int_o^t \frac{d^2\mu(\tau)}{d\tau^2} \frac{e^{\mu(\tau)}}{\left(\frac{d\mu(\tau)}{d\tau}\right)^2} \, d\tau \ . \qquad \text{(C.16)}$$

Since

$$\frac{d\mu(\tau)}{d\tau} = -s_{\prec} + j\omega_i(\tau) \qquad \text{(C.17)}$$

and

$$\frac{d^2\mu(\tau)}{d\tau^2} = j \frac{d\omega_i(\tau)}{d\tau} \ , \qquad \text{(C.18)}$$

the first term of (C.16) becomes

$$\left[\frac{e^{\mu(\tau)}}{\frac{d\mu(\tau)}{d\tau}}\right]_o^t = \frac{\exp\left[-s_\alpha t + j\int_o^t \omega_i(\tau)\,d\tau\right]}{-s_\alpha + j\omega_i(\tau)} - \frac{1}{-s_\alpha + j\omega_i(o)}\ , \quad (C.19)$$

and the second term of (C.16) becomes

$$\int_o^t \frac{d^2\mu(\tau)}{d\tau^2}\ \frac{e^{\mu(\tau)}}{d\mu(\tau)^2}\,d\tau = \int_o^t j\,\frac{d\omega_i(\tau)}{d\tau}\ \frac{\exp\left[-s_\alpha\tau + j\int_o^\tau \omega_i(\tau)\,d\tau\right]}{\left[-s_\alpha + j\omega_i(\tau)\right]^2}\,d\tau\ . \quad (C.20)$$

Therefore,

$$e_\alpha = A_\alpha e^{s_\alpha t}\left[\frac{\exp\left[-s_\alpha t + j\int_o^t \omega_i(\tau)\,d\tau\right]}{-s_\alpha + j\omega_i(t)} - \frac{1}{-s_\alpha + j\omega_i(o)}\right. \quad (C.21)$$

$$\left. + j\int_o^t \frac{d\omega_i(\tau)}{d\tau}\ \frac{\exp\left[-s_\alpha\tau + j\int_o^\tau \omega_i(\tau)\,d\tau\right]}{\left[-s_\alpha + j\omega_i(\tau)\right]^2}\,d\tau\right],$$

or

$$e_\alpha = A_\alpha\ \frac{\exp\left[j\int_o^t \omega_i(\tau)\,d\tau\right]}{-s_\alpha + j\omega_i(t)} - A_\alpha e^{s_\alpha t}\ \frac{1}{-s_\alpha + j\omega_i(o)} \quad (C.22)$$

$$+ A_\alpha e^{s_\alpha t}\ j\int_o^t \frac{d\omega_i(\tau)}{d\tau}\ \frac{\exp\left[-s_\alpha + j\int_o^\tau \omega_i(\tau)\,d\tau\right]}{\left[-s_\alpha + j\omega_i(\tau)\right]^2}\,d\tau\ .$$

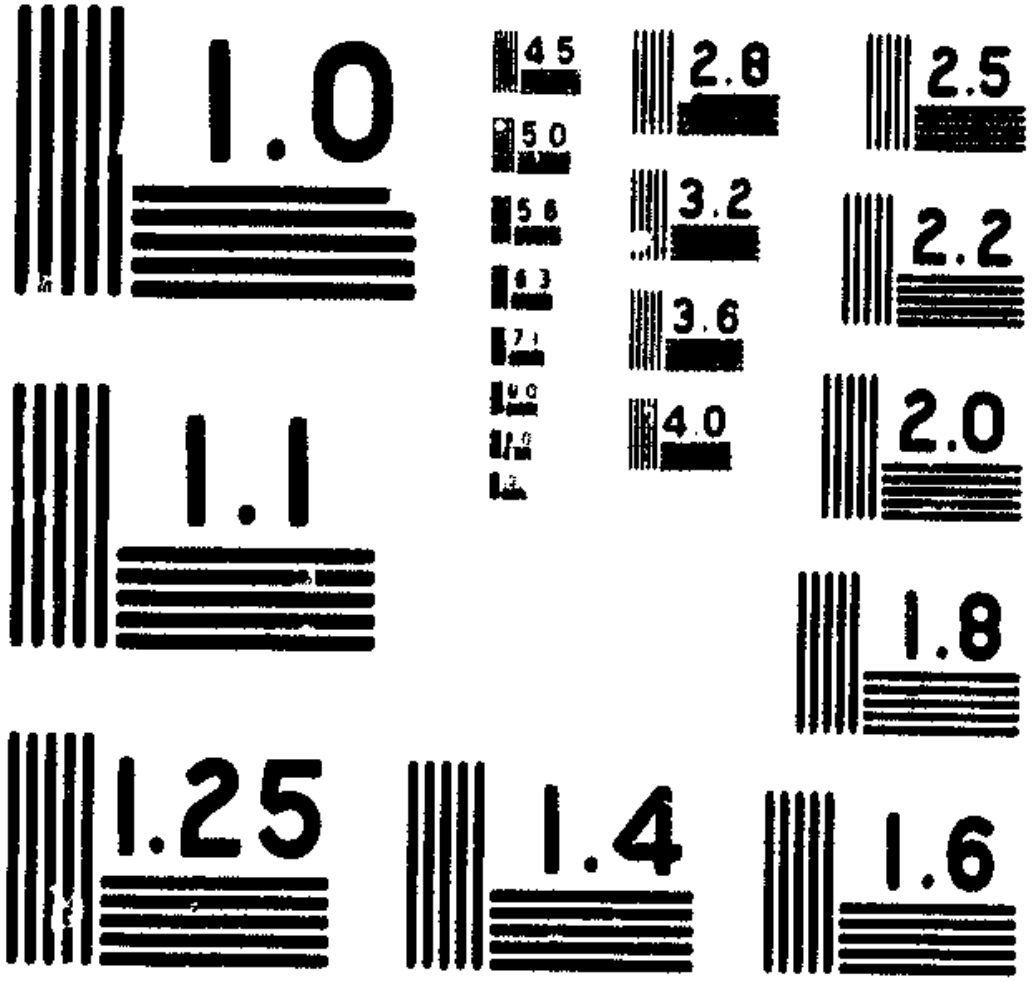

MICROCOPY RESOLUTION TEST CHART

NATIONAL BUREAU OF STANDARDS - 1963

The steady-state response to a sinusoidal input can now be found. The second term in (C.22) is the transient term which tends to zero as t gets large, provided that the real part of s_α is negative for all α. For a stable network, this is true since all poles are located in the left-half plane. The third term is negligible if

$$\left| \frac{\frac{d\omega_i(\tau)}{d\tau}}{\left[-s_\alpha + j\omega_i(\tau)\right]^2} \right| \ll 1 \qquad (C.23)$$

for all α and τ. If this is true, we are left with the quasi-steady-state solution

$$e_\alpha(t) = A_\alpha \frac{\exp\left[j \int_o^t \omega_i(\tau)\, d\tau\right]}{-s_\alpha + j\omega_i(t)} , \qquad (C.24)$$

Since $e_o(t)$ is the sum of all $e_\alpha(t)$ terms

$$e_o(t) = \sum_\alpha A_\alpha \frac{\exp\ j \int_o^t \omega_i(\tau)\, d\tau}{-s_\alpha + j\omega_i(t)} , \qquad (C.25)$$

which may be written as

$$e_o(t) = \exp\left[j \int_o^t \omega_i(\tau)\, d\tau\right] \frac{A_\alpha}{-s_\alpha + j\omega_i(t)} . \qquad (C.26)$$

Referring to (C.3), (C.26) may be written as

$$e_o(t) = \exp\ j \int_o^t \omega_i(\tau)\, d\tau\ \ Y(\omega_i) , \qquad (C.27)$$

where it is understood that ω_i s a function of t.

If $Y(\omega_i)$ is represented as

$$Y(\omega_i) = \left|Y(\omega_i)\right| e^{j\phi(\omega_i)} , \tag{C.28}$$

then

$$e_o(t) = \left|Y(\omega_i)\right| \exp\left[j\int_o^t \omega_i(\tau)\, d\tau + \phi(\omega_i)\right] . \tag{C.29}$$

The term

$$\int_o^t \omega_i(\tau)\, d\tau$$

is the instantaneous input phase, which may be represented as

$$\int_o^t \omega_i(\tau)\, d\tau = \omega_c t + \theta(t) , \tag{C.30}$$

where ω_c is the nominal carrier frequency and $\theta(t)$ is the phase perturbation on that carrier. Using this substitution, (C.29) becomes

$$e_o(t) = \left|Y(\omega_i)\right| e^{j\left[\omega_c t + \theta(t) + \phi(\omega_i)\right]} . \tag{C.31}$$

If the network is such that

$$\left|Y(\omega_i)\right| = 1 \tag{C.32}$$

for all ω_i, then

$$e_o(t) = e^{j\left[\omega_c + \theta(t) + \phi(\omega_i)\right]} \tag{C.33}$$

for

$$e_i(t) = e^{j\left[\omega_c t + \theta(t)\right]} . \tag{C.34}$$

The assumption that this is true forms the basis for the analysis carried out in Chapters III and IV.

APPENDIX D

REPRESENTATION OF NARROW-BAND NOISE

In order to determine the effect of noise on a pilot signal, a representation of narrow-band noise is necessary. The commonly used representation developed in this appendix was first documented by S. O. Rice.[14]

The noise power density spectrum will be assumed to have the constant value N_o Watts per Hertz in the frequency band of interest. The noise voltage, n(t), will be approximated by a sum of sinusoids in the form

$$n(t) = \sum_{n=1}^{M} A_n \cos(\omega_n t + \theta_n) , \qquad (D.1)$$

where θ_n is a random variable with a uniform distribution between zero and 2π.

The value of the A_n's must be determined such that the mean-square value of (D.1), $\overline{n^2(t)}$, is equal to the total noise power, N, which is $N_o B$, where B is the noise bandwidth. The bandwidth, B, is assumed to be divided into M slots, each slot being Δf Hz wide. As illustrated in Figure D-1, each slot is replaced by a sinusoidal component having power equal to the noise power $N_o(\Delta f)$. Thus

$$\frac{A_n^2}{2} = N_o(\Delta f) \qquad (D.2)$$

or

$$A_n = \sqrt{2N_o(\Delta f)} \quad . \qquad (D.3)$$

Thus, (D.1) becomes

$$n(t) = \sum_{n=1}^{M} \sqrt{2N_o(\Delta f)} \cos(\omega_n t + \theta_n) \quad . \qquad (D.4)$$

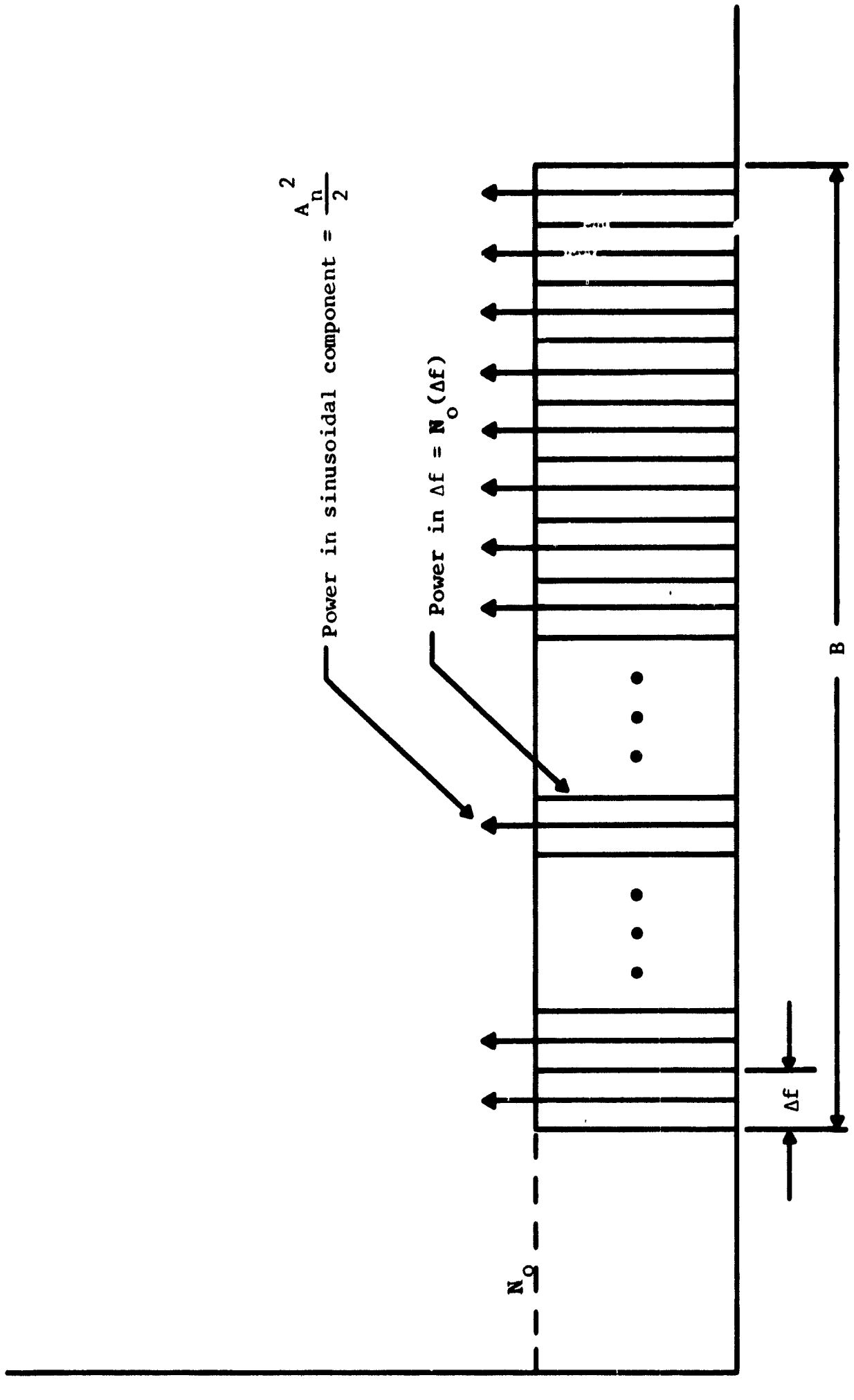

Figure D-1 Representation of Narrow-band Noise

The above expression may be re-written in the form

$$n(t) = \sum_{n=1}^{M} \sqrt{2N_o(\Delta f)} \cos \left[(\omega_n - \omega_c) t + \theta_n + \omega_c t\right] . \qquad (D.5)$$

Applying the trigonometric identity

$$\cos (x + y) = \cos x \cos y - \sin x \sin y , \qquad (D.6)$$

(D.5) becomes

$$n(t) = \sum_{n=1}^{M} \sqrt{2N_o(\Delta f)} \cos \left[(\omega_n - \omega_c) t + \theta_n\right] \cos \omega_c t$$

$$-\sin \left[(\omega_n - \omega_c) t + \theta_n\right] \sin \omega_c t , \qquad (D.7)$$

or

$$n(t) = \cos \omega_c t \sum_{n=1}^{M} \sqrt{2N_o(\Delta f)} \cos \left[(\omega_n - \omega_c) t + \theta_n\right]$$

$$-\sin \omega_c t \sum_{n=1}^{M} \sqrt{2N_o(\Delta f)} \sin \left[(\omega_n - \omega_c) + \theta_n\right] . \qquad (D.8)$$

By defining

$$x_c(t) = \sum_{n=1}^{M} \sqrt{2N_o(\Delta f)} \sin \left[(\omega_n - \omega_c) + \theta_n\right] , \qquad (D.9)$$

and

$$x_s(t) = \sum_{n=1}^{M} \sqrt{2N_o(\Delta f)} \sin \left[(\omega_n - \omega_c) + \theta_n\right] , \qquad (D.10)$$

(D.8) becomes

$$n(t) = x_c(t) \cos \omega_c t - x_s(t) \sin \omega_c t \ . \qquad (D.11)$$

If n(t) is assumed narrow-band, the frequencies $\omega_n - \omega_c$ are small when compared to ω_c. Equations (D.9) and (D.10) show that, under this condition, $x_c(t)$ and $x_s(t)$ are random processes which are slowly varying when compared to cos $\omega_c t$. They are also independent since they are defined as a sum of sinusoids having random initial phase. (D.11) shows that the mean-square value of n(t) is

$$\overline{n^2(t)} = \frac{1}{2} \overline{x_c^2(t)} + \frac{1}{2} \overline{x_s^2(t)} \ , \qquad (D.12)$$

since $x_c(t)$ and $x_s(t)$ are independent and since the mean-square value of a sinusoid is 1/2. From (D.9) and (D.10) it can be seen that the mean-square values of $x_c(t)$ and $x_s(t)$ are equal. Thus

$$\overline{n^2(t)} = \overline{x_c^2(t)} = \overline{x_s^2(t)} = \sigma^2 , \qquad (D.13)$$

where σ^2 is the variance, or average noise power. Half of the noise power is in the in-phase component and half of the noise power is in the quadrature component.

Sometimes it is convenient to write (D.11) in the form

$$n(t) = X_c(t) \cos \omega_c t + X_s(t) \sin \omega_c t \ , \qquad (D.14)$$

where $X_c(t) = x_c(t)$ and $X_s(t) = -x_s(t)$. This eliminates the minus sign in (D.11). It is apparent that the statistics of $X_c(t)$ are identical with the statistics of $x_c(t)$ and $x_s(t)$.

APPENDIX E

EFFECT OF DEMODULATION ERRORS

Noise and other perturbations result in dynamic phase errors in the synthesized demodulation carrier. The effect of these errors is investigated for sinusoidal modulation in both DSB and SSB systems.[15]

A. Phase Errors in a DSB System

Assume that the data is of the form

$$e_m(t) = \cos \omega_m t, \tag{E.1}$$

which, after DSB modulation becomes

$$e_{DSB}(t) = \cos (\omega_n + \omega_m) t + \cos (\omega_n - \omega_m) t, \tag{E.2}$$

where ω_n represents the carrier frequency. The carrier is assumed sinusoidal with a peak amplitude of two to eliminate amplitude scaling. If $e_{DSB}(t)$ is demodulated using a synthesized carrier of the form

$$e_{sc}(t) = \cos \left[\omega_n t + \phi(t)\right], \tag{E.3}$$

the result, after filtering out the $2\omega_n$ terms, is

$$\begin{aligned} e_d(t) = {} & \frac{1}{2} \cos \left[\omega_m t - \phi(t)\right] \\ & + \frac{1}{2} \cos \left[-\omega_m t - \phi(t)\right], \end{aligned} \tag{E.4}$$

or

$$e_d(t) = \cos \phi(t) \cos \omega_m t . \tag{E.5}$$

In the above expression $\phi(t)$ is a dynamic phase error which introduces an amplitude modulation in the desired signal, $\cos \omega_m t$. The problem now is to determine the rms error between the actual and desired signals when the rms value of $\phi(t)$ is known.

The first step in this process is to define an error signal, $\varepsilon(t)$, as

$$\varepsilon(t) = \cos \omega_m t \left[1 - \cos \phi(t)\right] \tag{E.6}$$

and determine the mean-square value of $\varepsilon(t)$. For small values of $\phi(t)$, the approximation

$$1 - \cos \phi(t) \approx \frac{1}{2} \phi^2(t) \tag{E.7}$$

can be made. This yields

$$\varepsilon(t) = \frac{1}{2} \phi^2(t) \cos \omega_m t, \tag{E.8}$$

from which the mean-square value of $\varepsilon(t)$, $\overline{\varepsilon^2(t)}$, can be obtained. Assume $\phi(t)$ to be a Gaussian random variable with zero mean and variance σ_ϕ^2. Under these conditions, the probability density function, $p(\phi)$, describing $\phi(t)$, can be written as

$$p(\phi) = \frac{1}{\sqrt{2\pi}\,\sigma_\phi} e^{-\phi^2/2\sigma_\phi^2}. \tag{E.9}$$

The mean square value of $\phi^2(t)$ can be found by introducing a second random variable, ξ, defined as

$$\xi = \phi^2(t), \tag{E.10}$$

The density function[16] for ξ is

$$p(\xi) = \frac{1}{\sigma_\phi \sqrt{2\pi\xi}} e^{-\xi/2\sigma_\phi^2} . \qquad (E.11)$$

The mean-square value of ξ is

$$\overline{\xi^2(t)} = \frac{1}{\sigma_\phi \sqrt{2\pi}} \int_0^\infty \xi^{3/2} e^{-\xi/2\sigma_\phi^2} d\xi , \qquad (E.12)$$

which, using (E.10) becomes,

$$\xi^2(t) = \frac{1}{\sigma_\phi \sqrt{2\pi}} \int_0^\infty \phi^3 e^{-\phi^2/2\sigma_\phi^2} 2\phi \, d\phi . \qquad (E.13)$$

The integral in (E.13) may now be evaluated to yield

$$\overline{\xi^2(t)} = 3\sigma_\phi^4 . \qquad (E.14)$$

Equation (E.8) may be written as

$$\varepsilon(t) = \frac{1}{2} \xi(t) \cos \omega_m t . \qquad (E.15)$$

Therefore, the mean-square value of $\varepsilon(t)$ is

$$\overline{\varepsilon^2(t)} = \frac{1}{8} \overline{\xi^2(t)} , \qquad (E.16)$$

since the mean-square value of a sinusoid is 1/2. Substitution of (E.15) into (E.16) yields

$$\overline{\varepsilon^2(t)} = \frac{3}{8}\,\sigma_\phi{}^4 \quad . \tag{E.17}$$

The rms error in the demodulated waveform is then given by

$$\varepsilon_{rms}(t) = \sqrt{\overline{\varepsilon^2(t)}} = 0.612\,\sigma_\phi{}^2 \quad . \tag{E.18}$$

B. Phase Errors in an SSB System

Assuming sinusoidal upper-sideband modulation, the SSB signal is given by

$$e_{SSB}(t) = \cos\,(\omega_n + \omega_m)\,t \quad , \tag{E.19}$$

which when multiplied by the carrier given by (E.3) yields

$$e_d = \cos\left[\omega_m t - \phi(t)\right] \quad . \tag{E.20}$$

Re-writing this expression yields

$$e_d(t) = \cos\,\omega_m t\,\cos\,\phi(t) + \sin\,\omega_m t\,\sin\,\phi(t) \quad . \tag{E.21}$$

The error signal is then given by

$$\varepsilon(t) = \cos\,\omega_m t - \cos\,\phi(t)\,\cos\,\omega_m t - \sin\,\omega_m t\,\sin\,\phi(t) \quad , \tag{E.22}$$

which, for small $\phi(t)$, may be approximated as

$$\varepsilon(t) = -\phi(t)\,\sin\,\omega_m t \quad . \tag{E.23}$$

Thus, for the SSB case, the mean square error is

$$\overline{\varepsilon^2(t)} = \frac{1}{2}\,\sigma_\phi^{\,2} \quad , \tag{E.24}$$

and the rms error is

$$\varepsilon_{rms}(t) = \sqrt{\overline{\varepsilon^2(t)}} = 0.707\ \sigma_\phi \quad . \tag{E.25}$$

Equations (E.18) and (E.25) are plotted in Figure E-1. It is clear that phase errors in the demodulation carrier are much more serious in an SSB system than in a DSB system.

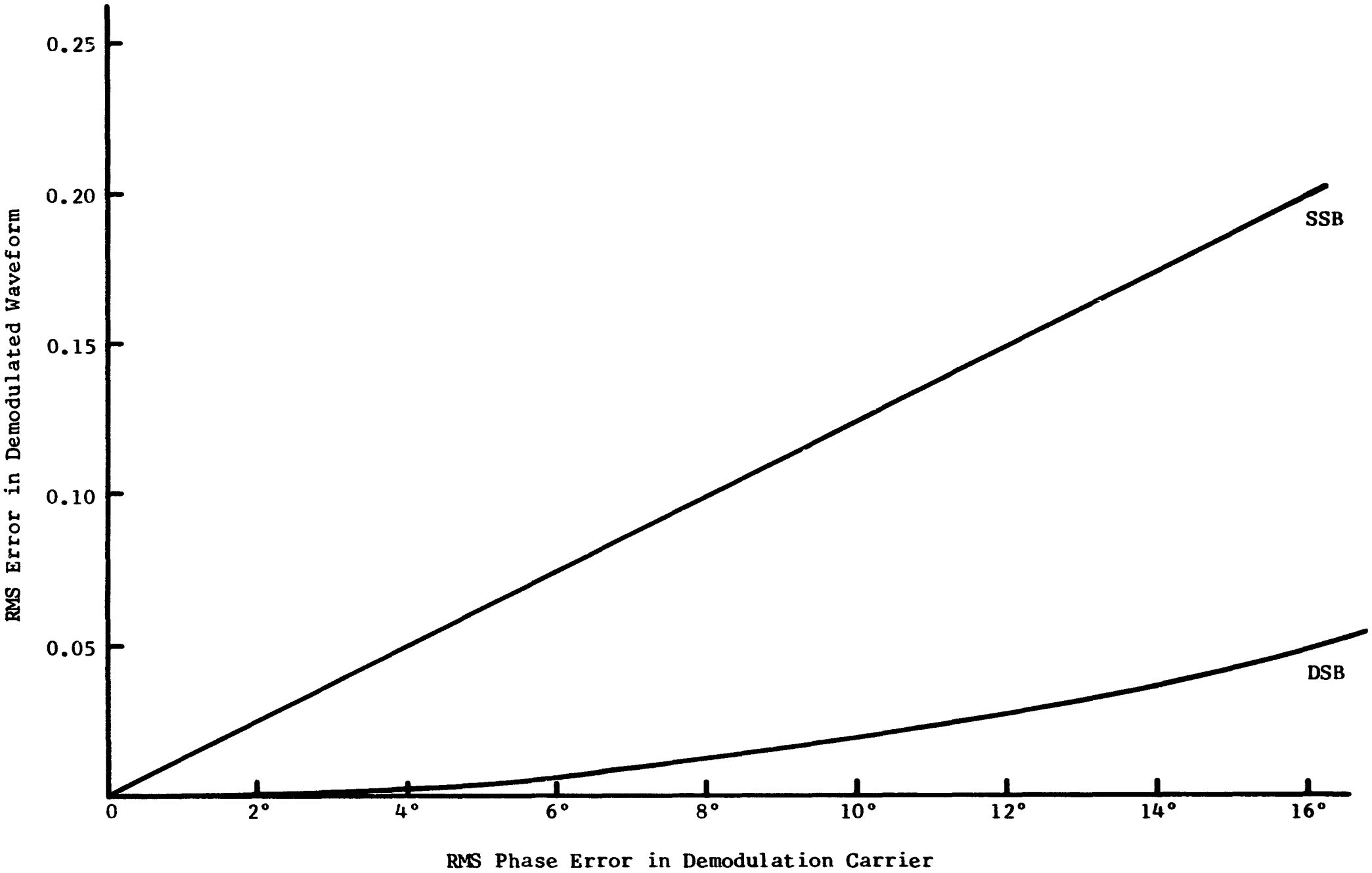

Figure E-1 RMS Error for SSB and DSB

REFERENCES

1. Chao, S. C., "Flutter and Time Errors in Magnetic Data Recorders," Proceedings of the International Telemetering Conference, Vol. 1, 1965, p. 582.

2. Schwartz, M., Bennett, W. R., and Stein, S., Communication Systems and Techniques, McGraw-Hill Book Company, Inc., New York, 1966, pp. 229-232.

3. Rice, S. O., "Statistical Properties of a Sine Wave Plus Random Noise," Bell System Technical Journal, Vol. 27, January, 1948, pp. 109-157.

4. Hancock, J. C., An Introduction to the Principles of Communication Theory, McGraw-Hill Book Company, Inc., New York, 1965, pp. 133-136.

5. Panter, Philip F., Modulation, Noise, and Spectral Analysis, McGraw-Hill Book Company, Inc., New York, 1965, pp. 164-169.

6. Hancock, op. cit., p. 136.

7. Simpson, R. S., and Davis, R. C., "Tape Recorder Flutter Analysis and Bit-Rate Smoothing of Digital Data," University of Alabama, Bureau of Engineering Research, June, 1966, pp. 4-12.

8. Baghdady, Elie J., "Theory of Low Distortion Reproduction of FM Signals in Linear Systems," IRE Transactions on Circuit Theory, Vol. CT-5, No. 3, September, 1958, p. 202.

9. Carson, J. R., and Fry, T. C., "Variable-Frequency Electrical Analysis," Bell System Technical Journal, Vol. 16, October, 1937, pp. 513-540.

10. Van der Pol, B., "The Fundamental Principles of Frequency Modulation," Journal of the Institution of Electrical Engineers, Vol. 93, Part 3, May, 1946, pp. 153-158.

11. Stumpers, F. L. H. M., "Distortion of Frequency-Modulated Signals in Electrical Networks," Communication News, Vol. 9, April, 1948, pp. 82-92.

12. Baghdady, op. cit., pp. 202-214.

13. Morley, G. A., "Phase Delay Variations in an FM Receiver," Canadian Armament Research and Development Establishment Technical Memorandum 344/60, July, 1960.

14. Rice, loc. cit.

15. Nichols, M. H. and Rauch, L. L., "Telemetry," USAF Report No. ESD-TR-66-464, July, 1966, pp. 7-70.

16. Papoulis, A., Probability, Random Variables, and Stochastic Processes, McGraw-Hill Book Company, Inc., New York, 1965, p. 130.

BIBLIOGRAPHY

BOOKS

Davenport, Wilber B., Jr., and Root, William L., An Introduction to the Theory of Random Signals and Noise, McGraw-Hill Book Company, Inc., New York, 1958.

Davies, Gomer L., Magnetic Tape Instrumentation, McGraw-Hill Book Company, Inc., New York, 1961.

Hancock, J. C., An Introduction to the Principles of Communication Theory, McGraw-Hill Book Company, Inc., New York, 1961.

Harman, Willis W., Principles of the statistical Theory of Communication, McGraw-Hill Book Company, Inc., New York, 1963.

Panter, Philip F., Modulation, Noise, and Spectral Analysis, McGraw-Hill Book Company, Inc., New York, 1965.

Papoulis, A., Probability, Random Variables, and Stochastic Processes, McGraw-Hill Book Company, Inc., New York, 1965.

Rowe, Harrison E., Signals and Noise in Communication Systems, D. Van Nostrand Company, Inc., Princeton, New Jersey, 1965.

Schwartz, M., Bennett, W. R., and Stein, S., Communication Systems and Techniques, McGraw-Hill Book Company, Inc., New York, 1966.

ARTICLES, REPORTS AND PAPERS

Baghdady, Elie J., "Theory of Low-Distortion Reproduction of FM Signals in Linear Systems," IRE Transactions on Circuit Theory, Vol. CT-5, No. 3, pp. 202-214, September, 1958.

Carson, J. R., and Fry, T. C., "Variable-Frequency Electric Circuit Theory," Bell System Technical Journal, Vol. 16, pp. 513-540, October, 1937.

Chao, S. C., "Flutter and Time Errors in Magnetic Data Recorders," Proceedings of the International Telemetering Conference, Vol. 1, pp. 578-594, 1965.

Morley, G. A., "Phase Delay Variations in an FM Receiver," Canadian Armament Research and Development Establishment Technical Memorandum 344/60, July, 1960

Nichols, M. H., and Rauch, L. L., "Telemetry," USAF Report No. ESD-TR-66-464, July, 1966.

Ratz, Alfred G., "The Effect of Tape Transport Flutter on Spectrum and Correlation Analysis," IEEE Transactions on Space Electronics and Telemetry, Vol. SET-10, pp. 129-134, December, 1964.

Rice, S. O., "Mathematical Analysis of Random Noise," Bell System Technical Journal, Vol. 23, pp. 282-332, July, 1944.

Rice, S. O., "Mathematical Analysis of Random Noise," Bell System Technical Journal, Vol. 24, pp. 46-157, January, 1945.

Rice, S. O., "Statistical Properties of Sine Wave Plus Random Noise," Bell System Technical Journal, Vol. 27, pp. 109-157, January, 1948.

Simpson, R. S., and Davis, R. C., "Tape Recorder Flutter Analysis and Bit-Rate Smoothing of Digital Data," University of Alabama, Bureau of Engineering Research, June, 1966.

Simpson, R. S. and Tranter, W. H., "Effect of Recorder Flutter on Coherent Demodulation in an AM-Baseband System," Proceedings of the National Telemetering Conference, pp. 46-49, 1967.

Van der Pol, B., "The Fundamental Principles of Frequency Modulation," Journal of the Institution of Electrical Engineers, Vol. 93, Part III, pp. 153-158, May, 1946.

COMMUNICATION SYSTEMS GROUP

RECENT REPORTS

An Exponential Digital Filter for Real Time Use, R. S. Simpson, C. A. Blackwell and W. H. Tranter, July, 1965.

An Evaluation of Possible Modifications of the Existing IRIG FM/FM Telemetry Standards, R. S. Simpson, C. A. Blackwell and J. B. Cain, May, 1966.

Analysis of Premodulation Gain in a SS/FM Telemetry System, R. S. Simpson and C. A. Blackwell, June, 1966.

Tape Recorder Flutter Analysis and Bit-Rate Smoothing of Digital Data, R. S. Simpson and R. C. Davis, June, 1966.

A Study of Redundancy in Saturn Flight Data, R. S. Simpson and J. R. Haskew, August, 1966.

AM-Baseband Telemetry Systems, Vol. 1: Factors Affecting a Common Pilot System, R. S. Simpson and W. H. Tranter, February, 1968.